Vibrational Strong Coupling in Cavity QED forms a Macroscopic Quantum State

M. Elious Mondal,[1] Sebastian Montillo Vega,[1] and Pengfei Huo[1, 2, 3, *]

[1] *Department of Chemistry, University of Rochester, 120 Trustee Road, Rochester, NY 14627, USA*
[2] *The Institute of Optics, Hajim School of Engineering, University of Rochester, Rochester, NY 14627, USA*
[3] *Center for Coherence and Quantum Science, University of Rochester, Rochester, New York 14627, USA*

Recent experiments demonstrated the possibilities of modifying ground-state chemical reaction rates by placing an ensemble of molecules in an optical microcavity. A strong collective, resonant coupling between the cavity mode and molecular vibrations forms vibration-polaritons. This regime is commonly referred to as Vibrational Strong Coupling (VSC), and typically operates in the *absence* of any light source ("in the dark"). VSC causes reaction rate constant modifications, exhibits phase-transition type of behavior for equilibrium constant modifications, and the effect starts only when the collective Rabi splitting surpasses a threshold. Existing theoretical work often focuses on the single excitation pictures, centered around the idea of vibrational polaritons and dark states. We found that due to the many-body nature of VSC, most of the VSC effects could be potentially explained by forming a macroscopic condensation of Bogoliubov quasiparticles, commonly referred to as Bogolon. We theoretically demonstrate that by surpassing a critical Rabi splitting, the VSC system starts to macroscopically occupy *one* Bogolon condensate state, which we believe is the common explanation for VSC-induced effects.

INTRODUCTION

Collective coupling between matter excitations with photonic excitations inside an optical cavity forms polaritons [1], a quasi-particle that is a superposition of both types of excitations. This field is often referred to as cavity quantum electrodynamics (QED) [2–4], with the focus on investigating the fundamental properties of polaritons and how to control them. Historically, the field has focused on exciton-polaritons [5–7] by coupling optical transitions of materials to cavity photonic excitations, including atoms [4], moleucles [5–10], and solid-state materials [11, 12]. Very recently (since 2015), Ebbesen [13, 14] and Simpkins [15] have independently achieved the vibrational strong coupling (VSC) condition in cavity QED, by coupling the vibrational transition to an IR cavity mode, forming vibrational polaritons. Since then, there are a lot of intriging phenomena reported under VSC, most of them are operating *without* any optical pumping (under the dark [16]), and exhibit change of ground state chemical reaction rate constants, suppression [17–21] or enhancement [22–24], typically by 4-5 times. Note that these experiments are fundamentally different than those that use external lasers to probe the vibrational polaritons and single-excitation subspace [25, 26], which can be theoretically explained [26–29]. The VSC under the dark has also been shown to selectively slow down one reaction out of two competing reactions [30], thus tilting the selectivities of two competing reactions [31]. VSC has also been shown to change the equilibrium constant for charge transfer complexation reaction [32], for confirmational changes of chemical complex [33], and exhibit a phase transition type of behavior for the equilibrium constant upon changing the molecular concentration [32, 33]. Similar phase transition-type behavior is also observed in the VSC-induced polymerization experiments [34–37]. It was also speculated that the vibrational point group symmetry played a crucial role in the system to exhibit the VSC effect [38]. VSC has also been shown to significantly enhance the electrical conductance through originally non-conducting polymers [39]. Since there is no external pumping in these VSC experiments, it was speculated that the "zero-point-vacuum field fluctuation" must be responsible for the observed effects [17].

While the experimental mysteries keep piling up, there is no well-accepted theoretical explanation [40, 41] for all of the above-mentioned VSC effects, despite progress on the VSC-induced rate constant modification theories for a few-molecule coupled to the cavity [42–56], on VSC-influenced electron transfer reactions [57, 58], and for a very special model of collective coupling between cavity mode, solvent, and reaction coordinate [59–61]. The most challenging effect to explain is indeed the *collective coupling* effect: how does weak light-matter coupling per vibration even modify chemical reactivities and properties? So far, neither classical Transition State Theory [42, 62–65] (or beyond classical rate theory [66]) nor quantum dynamics simulations [52] (under the meanfield limit [67]) could explain this effect, but there are interesting hypotheses to demonstrate the collectiveness in VSC [21, 27, 29, 44, 52, 57, 59–61, 68–79], typically for $N \approx 2 \sim 10^3$ vibrations collectively coupled to the cavity.

Collective light-matter couplings are commonly described by the Tavis-Cummings Hamiltonian [80] as follows

$$\hat{H} = \sum_{n=1}^{N} \hbar\omega_n \hat{\sigma}_n^\dagger \hat{\sigma}_n + \hbar\omega_c \hat{a}^\dagger \hat{a} + \sum_{n=1}^{N} \hbar g_n \left[\hat{\sigma}_n^\dagger \hat{a} + \hat{a}^\dagger \hat{\sigma}_n\right], \tag{1}$$

where N emitters are collectively coupled to a cavity

* pengfei.huo@rochester.edu

mode described by $\{\hat{a}^\dagger, \hat{a}\}$ under the rotating wave approximation. For the emitter, one often approximate them as a two-level system, $\{|\mathrm{g}_n\rangle, |\mathrm{e}_n\rangle\}$, and have $\hat{\sigma}_n^\dagger = |\mathrm{e}_n\rangle\langle \mathrm{g}_n|$, and $\hat{\sigma}_n = |\mathrm{g}_n\rangle\langle \mathrm{e}_n|$. Further, ω_n is the emitter frequency for emitter n and g_n is the light-matter coupling strength between this emitter and the cavity mode. More commonly, one assumes that $\omega_n = \omega_0$, and $g_n = g_\mathrm{c}$ without any disorders in emitter frequency and in light-matter coupling strength [80]. In the single excitation subspace, one has

$$\hat{a}^\dagger|0\rangle \equiv |\mathrm{g}\rangle \otimes |1_\mathrm{ph}\rangle, \quad \hat{\sigma}_n^\dagger|0\rangle = |\mathrm{e}_n\rangle \otimes |0_\mathrm{ph}\rangle,$$

where $|0\rangle$ is the TC vacuum state without any excitations, and $|0_\mathrm{ph}\rangle$ is the zero photon state. With symmetry $\omega_n = \omega_0$ and $g_n = g_\mathrm{c}$ (no disorders), and under the resonance condition $\omega_c = \omega_0$, there are two *optically bright* polariton states

$$|\pm\rangle = \frac{1}{\sqrt{2}}\Big[\hat{a}^\dagger \otimes \hat{\mathcal{I}}_\sigma \pm \frac{1}{\sqrt{N}}\sum_{n=1}^{N} \hat{\sigma}_n \otimes \hat{\mathcal{I}}_a\Big]|0\rangle, \qquad (2)$$

where $\hat{\mathcal{I}}_\sigma$ and $\hat{\mathcal{I}}_a$ are identities in the matter and photonic subspace, respectively. The eigenenergies associated with $|\pm\rangle$ are $E_\pm = \hbar\omega_0 \pm \sqrt{N}g_\mathrm{c}$, and there is an energy splitting, commonly referred to as the Rabi splitting Ω_R, expressed as

$$\Omega_\mathrm{R} = 2\sqrt{N}g_\mathrm{c}, \qquad (3)$$

and a $N-1$ degenerated, optically dark (zero transition dipole from the ground state) states $\{|\mathcal{D}_j\rangle\}$ with the original energy of emitter $E_\mathcal{D} = \hbar\omega_0$. The system achieves strong coupling condition when

$$\Omega_\mathrm{R} > (\kappa + \gamma)/2, \qquad (4)$$

with γ as the matter linewidth and κ as the cavity linewidth. This means that one will be able to observe the splitting of the original one peak as two peaks in linear spectra [81].

The key challenge for any theory to explain the VSC effect (without any external laser pumping) is that the light-matter coupling strength g_c is very weak, and only the collective light-matter coupling is large, typically reported by the Rabi splitting $\Omega_\mathrm{R} = 2\sqrt{N}g_\mathrm{c}$ measured from linear optical spectra. Typically [82], $N \approx 10^6 - 10^{12}$, and $\Omega_\mathrm{R} \approx 100$ cm^{-1}, hence $g_\mathrm{c} \approx 5\times10^{-5} - 5\times10^{-2}$ cm^{-1}. As a reference, room temperature thermal energy is $k_\mathrm{B}T \approx 200$ cm^{-1} ≈ 26 meV. How was such a collective, delocalized light-matter coupling influence local chemical bond breaking, while the local light-matter coupling strength g_c is so weak? Another theoretical challenge to understand the VSC effect is that if one uses the single excitation picture mentioned above, then the $N-1$ dense manifold of dark vibrational polariton states should dominate and diminish all of the interesting VSC kinetics effects from the polariton states. The energy gap between $|\pm\rangle$ and dark states is only $\Omega_\mathrm{R}/2 \approx 50$ cm^{-1}, and the effective free energy for the dark states is lowered due to the entropic contribution from the dark state degeneracy, which is $k_\mathrm{B}T\ln(N-1) \approx 2760 - 5520$ cm^{-1} (for $N = 10^6 - 10^{12}$), making the dark states the most stable configuration in terms of free energy [83]. So one should expect that the dark state becomes the dominant manifold of states, and the chemical properties, including the reactivities and rate constant, should be identical to the outside cavity case.

The above-mentioned single excitation subspace pictures are largely borrowed from the excitonic/electronic strong coupling (ESC) case, and the mechanistic discussions are largely centered around the vibrational polaritons and dark states. However, we realize that ESC and VSC systems have *very different* energy scales, compared to $k_\mathrm{B}T$. The key difference is the emitter frequency. For ESC, optical transition has a typical value of $\hbar\omega_0 \sim 2$eV, and for VSC, $\hbar\omega_0 \approx 1000$ cm^{-1} ≈ 130 meV. This means that under room temperature, the Boltzmann probability for the excitonic system to be in the excited state is $\bar{n}/N = e^{-\beta\hbar\omega_0} \approx e^{-77} \approx 10^{-34}$, and for the range of N effectively coupled to each radiation mode in the cavity QED, no molecules are in the excited states unless there is a laser excitation, and the single excitation/few excitaton picture (polariton and dark states) is indeed a good mechanistic picture. On the other hand, for VSC, the Boltzmann probability for the vibrational DOF to be in the excited state is $\bar{n}/N = e^{-\beta\hbar\omega_0} \approx e^{-5} \approx 6.7\times10^{-3}$, so as large as 1/1000. For $N = 10^6$ molecules, that means $\bar{n} = 10^3$ of them are already in the excited states, due to the thermal distribution, and for $N = 10^{12}$ molecules, that means $\bar{n} = 10^9$ molecules are in the vibrationally excited states. As such, using the single/few excitation subspace picture in VSC is not appropriate. Upon coupling $N = 10^{12}$ molecular vibrations to the cavity, one in principle needs to consider up to the billionth excitation subspace!

The above revelation made us realize that the key to unraveling the VSC mysteries lies in describing the many-body physics of it, not in the superposition of a one-excitation (one-body) picture described in Eq. 2. In many-body physics, the condensed matter physics community has already provided well-established theories to understand intriguing phenomena, such as superfluidity and superconductivity. Weakly interacting bosonic particles can condense into one macroscopic state (bosonic coherence state) [84], which eventually explains the superfluidity [85]. Weak interactions between pairs of electrons with lattice phonon vibrations cause Cooper pairs to condense into a macroscopic state (Cooper pair coherence state), through the celebrated Bardeen–Cooper–Schrieffer (BCS) mechanism [86, 87], which eventually explained the superconductivity (under the normal regime, the phonon-mediated kind). As such, it is possible that weak light-matter couplings between the cavity mode and vibrations lead to effective interactions between two vibrations (phonons), and these many-body interactions lead to a new macroscopic state

(just like the coherence states in BCS or BEC), such that the VSC cavity QED system is dominated by that *one* macroscopic state at *room temperature*. We thus conjecture that in VSC, there are Bogoliubov quasiparticles, commonly referred to as Bogolon (see Eq. 32, which is the Bogoliubov transformed phonon creation and annihilation operators), condensed into one macroscopic state (under certain critical conditions) that dominates the behavior of the VSC systems and causes the mysterious effects observed experimentally [17, 33]. As such, we believe that vibrational Polaritons do not give the correct mechanistic picture to understand VSC-induced effects when there is no external laser pumping; rather, the Bogolons and their macroscopic condensation into one state do.

In this work, we theoretically demonstrate that the weak interaction of vibrations and the cavity mode $\sum_{n=1}^{N} \hbar g_n \left[\hat{\sigma}_n^\dagger \hat{a} + \hat{a}^\dagger \hat{\sigma}_n\right]$ term in Eq. 1, causes effective interactions among all vibrational DOFs which occurs inside the cavity, using the Schrieffer-Wolff transform [88]. The resulting effective Hamiltonian (Eq. 11), is *mathematically isomorphic* to the BSC-type effective Hamiltonian [86, 89]. This revelation suggests that we can use the standard BCS variational procedure to find the macroscopic ground state (for Bogolon condensate), which we referred to as $|\widetilde{0}\rangle$ in Eq. 14. This macroscopic state is a *truly many-body state*, as opposed to the superposition of N-single-particle states in the single excitation subspace, expressed in Eq. 2.

We derived the energy gap equation, Eq. 29, indicating the energy is lowered *per Bogolon*. This energy lowering is due to the coherent interaction among N degrees of freedom. Using the gap equation, we further show that the macroscopic state $|\widetilde{0}\rangle$ is stable compared to the normal thermodynamic state (which contains many microscopic states), in terms of free energy (when considering the dense manifold of vibrational excitations in the system). This $|\widetilde{0}\rangle$ is also stable compared to the vacuum states of vibrations outside the cavity, in terms of both energy and free energy. Interestingly, in Ref. 33, it was speculated that "strong coupling of a significant fraction of the molecules at the onset of VSC appears to pull nearly all the molecules into one phase by dipolar interactions due to the zero-point field oscillations of the optical mode". Despite that there is early theoretical work that hypothesizes a phase transition behavior in VSC [72, 74, 90] or macroscopic condensation onto lower polariton upon laser driving for VCS and achieves BEC [91], none of them suggest that the key mechanism of VSC is due to the Bogolon condensation. Our theoretical analysis suggests that this "phase transition" corresponds to the normal phase to a macroscopic coherent state transition. Our work thus provides a concrete theoretical foundation to support that speculation 33.

We further derived simplified, analytic gap equations with approximations, giving rise to the condition in Eq. 47 under which the Bogolon condensation state is more stable in terms of free energy. Using detailed parameters from the Ebbesen NMR experiments, our theory provides a reasonable estimation of the critical Rabi splitting to achieve the condensate phase that agrees with the experimental values. Our theory predicts that the critical value of the Rabi splitting scales as $\Omega_{\mathrm{R}} \propto \sqrt{\hbar\omega_0 + k_{\mathrm{B}}T} \propto \sqrt{1/M}$, where M is the effective mass for the vibrational DOF, meaning that with lower vibrational frequency ω_0 and lower T it requires a smaller Rabi splittig to achieve the condensation (that has a square root scalings of T and ω_0. This prediction can be tested using the same Ebbesen NMR experimental setup, with isotope effects (replacing C-H vibrations to C-D vibrations) or substitutions (replacing C-H vibrations to C-F vibrations, which also have NMR signatures). We furhter use the gap equation to derive the reaction rate constant suppression factor k/k_0, and found that it scales quadratically with the experimental Rabi splitting, and it gives a quantitative agreement with the experimental data reported in Ref. [17, 18]. We believe that condensing to $|\widetilde{0}\rangle$ could be the common origin for all rate constant modifications, equilibrium constant modifications, and beyond.

RESULTS AND DISCUSSIONS

Effective Hamiltonian. We start with the TC Hamiltonian in Eq. 1. We assume that the molecular vibration will have a normalized lineshape function as

$$\mathcal{A}_\nu(\omega - \omega_0) = \frac{1}{N}\sum_n \delta(\omega - \omega_n), \tag{5}$$

such that $\int d\omega \mathcal{A}_\nu(\omega - \omega_0) = 1$. We define the mean frequency as

$$\omega_0 = \sum_n \omega_n / N, \tag{6}$$

This function usually peaks at the mean frequency ω_0 (peak frequency), with a Gaussian shape or Lorentzian shape (or the Vigot convolution between them). With the Gaussian lineshape,

$$\mathcal{A}_\nu(\omega - \omega_0) = \frac{1}{\sqrt{2\pi\sigma^2}} \exp\left[\frac{(\omega - \omega_0)^2}{2\sigma^2}\right]. \tag{7}$$

We define the light-matter detuning with each individual frequency as

$$\delta_n = \omega_n - \omega_{\mathrm{c}}. \tag{8}$$

Further, the light-matter coupling strength exhibits disorders [59, 60, 64, 81] due to the orientational disorders of the transition dipole vector with respect to the cavity field polarization direction

$$g_n = g_{\mathrm{c}} \cos\phi_n, \tag{9}$$

where ϕ_n is the angle between the transition dipole vector of the n_{th} molecule relative to the field polarization direction, and it was believed to be isotropic in

3D, such that $\langle \cos\phi_n \cdot \cos\phi_m \rangle = 1/3\delta_{nm}$. With disorders [81], the composition and energy of these states will change [69, 92] and will impact the optical spectra of polaritons [81, 92] and Rabi splitting [93, 94]. For example, with isotropic dipole angular disorder, the experimentally observed Rabi splitting is [81, 94] $\Omega_{\rm R}^{\rm exp} = 2\sqrt{N}g_{\rm c}/\sqrt{3}$. Frequency disorder, on the other hand, could potentially enlarge Rabi splitting [93, 94]. One thus has to be careful when using $\Omega_{\rm R}^{\rm exp}$ to extract $\Omega_{\rm R} = 2\sqrt{N}g_{\rm c}$.

Further, $\sigma_n^\dagger$ and σ_n satisfy the Pauli-matrix commutation relations

$$[\hat{\sigma}_n^\dagger, \hat{\sigma}_n] = \hat{\sigma}_n^z, \quad [\hat{\sigma}_n^\dagger, \hat{\sigma}_n]_+ = \hat{\mathcal{I}}_n \tag{10a}$$

$$[\hat{\sigma}_n^\dagger, \hat{\sigma}_m] = 0, \quad [\hat{\sigma}_m^\dagger, \hat{\sigma}_n]_+ = 0. \tag{10b}$$

These commutation relations (for hardcore bosons) are identical to those of Cooper pairs' in the BCS theory when only considering the single Bogolon excitation subspace.

To adiabatically integrate out the photonic DOF, $\hat{a}^\dagger$ and $\hat{a}$, we apply Schrieffer-Wolff transform [88] on the TC Hamilotnian (Eq. 1), and effectively performing $2^{\rm nd}$ order perturbative expansion in $\lambda_n = g_n/\delta_n$. Indeed, for VSC, $g_{\rm c} \approx 5\times10^{-5} - 5\times10^{-2}$ cm^{-1} (for $N = 10^6 - 10^{12}$ and $\Omega_{\rm R} = 100$ cm^{-1}), and $\lambda_n \ll 1$ as long as $\delta_n > 1$ cm^{-1}. We choose the generator $\hat{S} = \sum_{n=1}^N \lambda_n(\hat{\sigma}_n^\dagger\hat{a} - \hat{\sigma}_n\hat{a}^\dagger)$, and the Hamiltonian in Eq. 1 can be transformed as

$$e^{\hat{S}}\hat{H}e^{\hat{S}} = \hat{\mathcal{H}} + \mathcal{O}(\lambda^3),$$

with λ_n chosen to satisfy the SW transform criteria (see details in the Supplemental Materials). The resulting effective Hamiltonian is expressed as

$$\hat{\mathcal{H}} = \sum_{n=1}^N \hbar\tilde{\omega}_n\hat{\sigma}_n^\dagger\hat{\sigma}_n + \sum_{n\neq m} G_{nm}\hat{\sigma}_n^\dagger\hat{\sigma}_m, \tag{11}$$

and the re-normalized vibrational frequency is

$$\tilde{\omega}_n = \omega_n + g_n^2/\delta_n. \tag{12}$$

The effective interactions between two vibrational excitations are

$$G_{nm} = \frac{\hbar}{2}g_n g_m\left(\frac{1}{\delta_n} + \frac{1}{\delta_m}\right). \tag{13}$$

Note that G_{nm} is the effective interaction between $\hat{\sigma}_n^\dagger$ and $\hat{\sigma}_m^\dagger$ due to their coupling to $\hat{a}$. The physical picture of such effective all-to-all interaction is also crystal clear: due to the light-matter coupling temr, $\hat{\sigma}_n^\dagger|0\rangle \to \hat{a}^\dagger|0\rangle$ through the $g_n\hat{a}^\dagger\hat{\sigma}_n$ term, and $\hat{a}^\dagger|0\rangle \to \hat{\sigma}_m^\dagger|0\rangle$ through the $g_m\hat{\sigma}_m^\dagger\hat{a}$ term, thus effectively create a coupling term between n and m, with coupling strength expressed as the 2nd order perturbation expression. The analysis is valid when the perturbative parameter $\lambda_n = g_n/\delta_n \ll 1$, and will *breakdown* when $\delta_n = 0$. The effective magnitude $|G_{nm}|$ will become larger when the detuning δ_n and δ_m are reduced. This might be the key to explaining the VSC resonance condition, which often requires very sensitive matching of the cavity frequency with vibrational frequency $\omega_{\rm c} \approx \omega_0$. In the experiments, due to the mirror fluctuations [95, 96], the best one could say is $\delta_n \approx 10^{-1} \sim 1$ cm^{-1}, even for the "perfect" detuning that $\omega_{\rm c} \approx \omega_0 \sim 10^3$ cm^{-1}. As such, λ_n is a valid perturbaive parameter per site n. The effective Hamiltonian can be viewed as a special case of the effective BCS Hamiltonian [97–99] under the rotating-wave approximation. In addition, it is interesting to note that the effective Hamiltonian could also be viewed as a long-range random bond $X-Y$ model with random $Z-$field [100–103], the Lipkin-Meshkov-Glick Hamiltonian [104–107], or a spin-glass type of Hamiltonian [74, 108–111].

Macroscopic Bogolon Condensate State. We conjecture that the true ground state of $\hat{\mathcal{H}}$ is a many-particle, macroscopic state, which we denote as $|\widetilde{0}\rangle$. Because $\hat{\mathcal{H}}$ is mathematically isomorphic to the BCS effective Hamiltonian, we hypothesize that this should be the coherent state of many Boglons that has the same form as the Schrieffer ansatz in the BCS theory [86, 87]. We thus follow closely the standard procedure in the BCS theory [89]. The Schrieffer ansatz for such a many-body coherent state (BCS-type ground state) is expressed as

$$|\widetilde{0}\rangle = \prod_{n=1}^N (u_n + v_n\hat{\sigma}_n^\dagger)|0\rangle = \bigotimes_{n=1}^N |\phi_n\rangle, \tag{14}$$

where $|\phi_n\rangle = u_n|g_n\rangle + v_n|e_n\rangle$, and $|0\rangle \equiv |g_1\rangle\otimes|g_2\rangle\otimes\cdots\otimes|g_N\rangle$ is the zero-particle state for the effective Hamiltonian in Eq. 11 (without the photonic DOF, so it is different than what is expressed in Eq. 2), where u_n and v_n are variational parameters, satisfying $u_n^2 + v_n^2 = 1$ for all $n \in [1, N]$, which can be determined by the BCS variational procedure (or equivalently, through the Bogoliubov canonical transform, Eq. 32). Note that $|\widetilde{0}\rangle$ in Eq. 14 is a true many-body state that is in stark contrast to the single excitation state $|\pm\rangle$ in Eq. 2.

The expectation value of $\hat{\mathcal{H}}$ under $|\widetilde{0}\rangle$ is expressed as

$$\overline{\mathcal{H}} \equiv \langle\widetilde{0}|\hat{\mathcal{H}}|\widetilde{0}\rangle = \sum_n \hbar\widetilde{\omega}_n|v_n|^2 - \sum_{n\neq m} G_{nm}\cdot\Big(u_n v_m^* u_m^* v_n\Big). \tag{15}$$

As Schriffer noticed [87], the trial ansatz described in Eq. 14 does not have a fixed excitation number $\bar{n}$. Further, one needs to satisfy the normalization $|u_n|^2 + |v_n^2| = 1$ for all n. As such, one needs to perform the conditional minimization using the Lagrange multiplier method.

The expectation value for the phonon excitations is

$$\bar{n} \equiv \langle\widetilde{0}|\sum_n \hat{\sigma}_n^\dagger\hat{\sigma}_n|\widetilde{0}\rangle = \sum_n |v_n|^2 = \sum_n \frac{e^{-\beta\hbar\widetilde{\omega}_n}}{1+e^{-\beta\hbar\widetilde{\omega}_n}} \tag{16}$$
$$\approx N\int d\omega\mathcal{A}_\nu(\omega-\omega_0)e^{-\beta\hbar\omega} \approx N\cdot e^{-\beta\hbar\omega_0},$$

where $\bar{n}$ is the excitation expectation value (number of phonon excitations) at T and at a given N. Here, we explicitly assume that coupling molecules collectively does not change the thermodynamic distributions for the N vibrations.

The interesting fact is that when counting the total system with N vibrational DOF, we expect that overall they still satisfy the Boltzmann statistics

$$\sum_n |v_n|^2 = \sum_n \frac{e^{-\beta\hbar\widetilde{\omega}_n}}{1+e^{-\beta\hbar\widetilde{\omega}_n}} \tag{17}$$

But for the individual site n in the new BCS-state $|\widetilde{0}\rangle$, very likely

$$|v_n|^2 \neq \frac{e^{-\beta\hbar\widetilde{\omega}_n}}{1+e^{-\beta\hbar\widetilde{\omega}_n}}, \tag{18}$$

especially when $\omega_n \to \omega_c$ due to the large effective coupling G_{nm} (c.f. Eq. 13). We shall see later that this is indeed the case for systems with vibrational frequency disorders (such that $\omega_n \neq \omega_0$, see Fig. 1b).

With $\widetilde{\mathcal{H}}$ and $\bar{n}$ expressions, and following the standard [89] Schriffer variational procedure [86, 87] and performing the conditional minimization using the Lagrange multiplier method [89], we variationally minimize the following function

$$\widetilde{\mathcal{H}} = \overline{\mathcal{H}} - \mu\bar{n} + \sum_n E_n(|u_n|^2 + |v_n^2| - 1), \tag{19}$$

where the μ is the chemical potential of the phonons, and E_n is effectively the energy level for particle n, both are Lagrange multipliers. Setting the variational condition $\delta\widetilde{\mathcal{H}} = 0$ requires that

$$\frac{\partial\widetilde{\mathcal{H}}}{\partial u_n} = 0, \quad \frac{\partial\widetilde{\mathcal{H}}}{\partial v_n} = 0, \tag{20}$$

for all possible $n \in [1, N]$. This leads to the following to coupled equations

$$\begin{pmatrix} \hbar\widetilde{\omega}_n - \mu & \Delta_n \\ \Delta_n^* & -(\hbar\widetilde{\omega}_n - \mu) \end{pmatrix} \begin{pmatrix} u_n^* \\ v_n^* \end{pmatrix} = E_n \begin{pmatrix} u_n^* \\ v_n^*, \end{pmatrix} \tag{21}$$

where we have defined the gap Δ_n (for $n \neq m$) as

$$\Delta_n \equiv \sum_{m\neq n} G_{nm} u_m^* v_m. \tag{22}$$

Note that even though Eq. 21 looks formally like a single particle equation with 2 states, the coupling term Δ_n (see Eq. 22) contains all coefficients $\{u_m, v_m\}$ such that these equations (for different n) are coupled to each other, describing the many-body physics. This was the true genius of the BCS theory. Further, Δ_n coupling term opens up an energy gap for the single particle state.

The matrix equation in Eq. 21 has two eigenvalues $\pm E_n$, with E_n expressed as

$$E_n = \sqrt{(\hbar\widetilde{\omega}_n - \mu)^2 + \Delta_n^2}, \tag{23}$$

which describes the dispersion relation of Bogolons, with eigenvectors

$$u_n = \cos\theta_n, \quad v_n = \sin\theta_n \tag{24}$$

and the mixing angle is

$$\cos 2\theta_n = (\hbar\widetilde{\omega}_n - \mu)/E_n, \quad \sin 2\theta_n = \Delta_n/E_n. \tag{25}$$

The macroscopic ground state in Eq. 14 is expressed as

$$|\widetilde{0}\rangle = \prod_{n=1}^{N} (\cos\theta_n + \sin\theta_n \hat{\sigma}_n^\dagger)|0\rangle. \tag{26}$$

Equivalently, the coefficients in Eq. 24 can be expressed as

$$u_n^2 = \frac{1}{2}\left[1 + \frac{\hbar\widetilde{\omega}_n - \mu}{E_n}\right] = \frac{1}{2}\left[1 + \frac{\hbar\widetilde{\omega}_n - \mu}{\sqrt{(\hbar\widetilde{\omega}_n - \mu)^2 + \Delta_n^2}}\right] \tag{27a}$$

$$v_n^2 = \frac{1}{2}\left[1 - \frac{\hbar\widetilde{\omega}_n - \mu}{E_n}\right] = \frac{1}{2}\left[1 - \frac{\hbar\widetilde{\omega}_n - \mu}{\sqrt{(\hbar\widetilde{\omega}_n - \mu)^2 + \Delta_n^2}}\right] \tag{27b}$$

Similar to the BCS-ground state, this $|\widetilde{0}\rangle$ should also be a broken symmetry state that breaks the local $U(1)$ symmetry, caused by the Higgs-type mechanism (when the gauge field consumes the Goldstone boson) [89].

Further, we want to obtain the explicit expression of the gap equation. Notice that

$$u_n^* v_n = \cos\theta_n \sin\theta_n = \frac{1}{2}\sin 2\theta_n = \frac{\Delta_n}{2E_n}, \tag{28}$$

together with the definition of Δ_n in Eq. 22, one can derive the celebratory BCS-type gap equation as follows

$$\Delta_n = \sum_{m\neq n} G_{nm} \cdot \frac{\Delta_m}{2E_m} = \sum_{m\neq n} \frac{G_{nm}\Delta_m}{2\sqrt{(\hbar\widetilde{\omega}_m - \mu)^2 + \Delta_m^2}}. \tag{29}$$

Further, we have a second complementary equation

$$\bar{n} = \sum_n v_n^2 = \sum_{n=1}^{N} \frac{1}{2}\left[1 - \frac{\hbar\widetilde{\omega}_n - \mu}{\sqrt{(\hbar\widetilde{\omega}_n - \mu)^2 + \Delta_n^2}}\right]. \tag{30}$$

For a given VSC system, T, N are fixed, and $\bar{n}$ should also be fixed (through Eq. 17). As such, one can numerically solve (thanks to more advacned computing powers nowadays compared to the BCS [86, 87] era in 1957) for μ and Δ_n from Eq. 29 and Eq. 30, which allows one to determine all $\{u_n, v_n\}$ in Eq. 41 and thus the new ground state $|\widetilde{0}\rangle$ in Eq. 14. Alternatively, one could focus on solving the coupled eigen equations in Eq. 21. Note that for diagonalizing the eigen equation (Eq. 21 associated with n, it requires the knowledge of other $\{u_m, v_m\}$ to compute Δ_n (see Eq. 29), and Eq. 21 thus needs a self-consistent field (SCF) solution, very similar to the case of Hartree-Fock

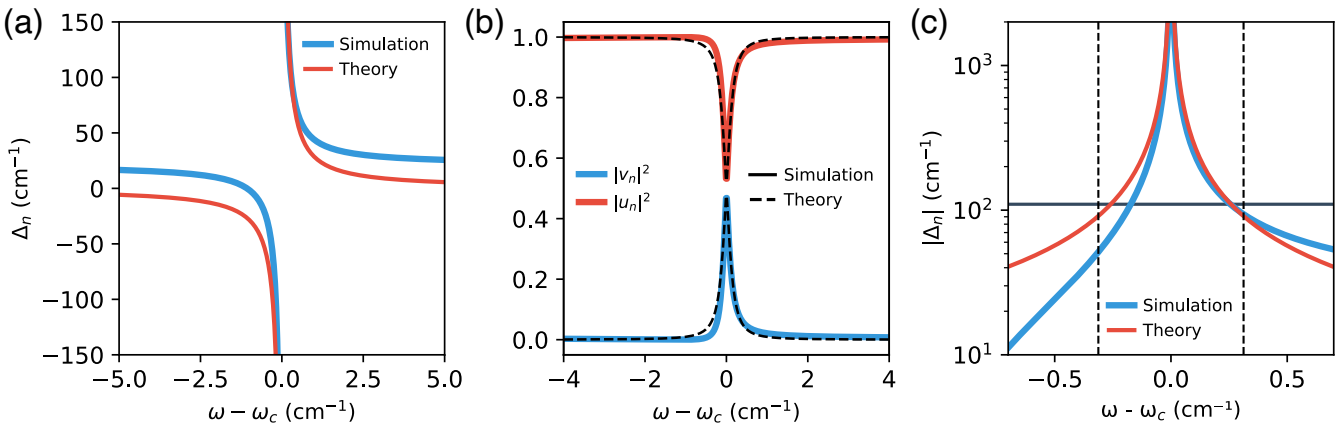

FIG. 1. **Numerical Simulation compared to the Analytic theory**. Here, we consider a system with $\omega_0 = 1000$ cm^{-1}, $\Omega_{\mathrm{R}} = 50$ cm^{-1}, $\omega_0 - \omega_c = 1$ cm^{-1}, $N = 10^7$ and $\sigma = 20$ cm^{-1}. (**a**) The numerical gap Δ_n (blue) and the analytic expression $\Delta(\omega)$ in Eq. 36. Note that the energy contribution will be $\sim \Delta_n u_n v_n$, so the changing sign of Δ_n will be compensated by the changing sign of $u_n v_n$, such that the $|\widetilde{0}\rangle$ state's energy will be lowered. (**b**) The expansion coefficients $|u_n|^2$ (red) and $|v_n|^2$ (blue), as a function of the detuning, obtained from numerical simulation (solid line) and analytic expression (black dashed) using Eq. 41. (**c**) The absolute value of gap, $|\Delta_n|$ obtained numerically (blue) and using Eq. 36 (red), with the black horizontal line indicating the value of $\sqrt{e^{-\beta\hbar\omega_0}}(\hbar\omega_0 + k_{\mathrm{B}}T)$. Above the blackline is the gap that satisfies the condition in Eq. 48. Two vertical dashed lines indicate the critical frequency ω_{c}^- and ω_{c}^+ based on Eq. 49.

theory in electronic structure. One could, in principle, provide the initial guess $\{u_n, v_n\}$, which could simply be the Boltzmann probability, then compute all Δ_n using Eq. 22, then solve Eq. 21 again, iteratively (with the constrains in Eq. 19), untill certian threshhold (say the changes in $\{|u_n|^2, |v_n|^2\}$ between two ajdecent iterations is smaller than a threshhold) is reached. A lot of useful techniques in the field of electronic structure that handle similar SCF procedures could be borrowed to solve our equations.

Fig. 1 presents our numerical simulation to solve Eq. 29 and Eq. 30. Here, we minimized by iterating a fixed-point map [112] on the global $g_m u_m^* v_m$ parameters, enforcing the expectation value for the phonon excitation number to be constrained at the Boltzmann distribution value (Eq. 16) at each step via monotone bisection for μ with linear mixing and small-detuning regularization for robustness. We consider a model system with $\omega_0 = 1000$ cm^{-1}, $\Omega_{\mathrm{R}} = 50$ cm^{-1}, $\omega_0 - \omega_c = 1$ cm^{-1}, $N = 10^7$ and $\sigma = 20$ cm^{-1}. Fig. 1 presents the numerically computed gap Δ_n as a function of $\omega_n - \omega_{\mathrm{c}}$ (blue curve), indicating the peaking behavior of the gap at the frequency close to ω_{c}. Fig. 1b presents the numerically obtained $|u_n|^2$ (red) and $|v_n|^2$ (blue), and indeed, when ω_n is close to the ω_{c}, these probability significantly deviate from the original Boltzmann probabilities. Note that these "hot spots" are in the frequency domain for Bogolongs, which are many-body collective excitations. And still, the overall statistics for N molecules satisfied the Boltzmann distribution (Eq. 17), as the constraint (the $-\mu\bar{n}$ part in Eq. 19) is explicitly enforced in our calculations.

We note that the same eigenequation (Eq. 21) and eigenvalue (Eq. 23) can also be obtained from the Bogoliubov transform [84, 89],

$$\begin{pmatrix} \hat{b}_n \\ \hat{b}_n^\dagger \end{pmatrix} = \begin{pmatrix} u_n & -v_n \\ v_n^* & u_n^* \end{pmatrix} \begin{pmatrix} \hat{\sigma}_n \\ \hat{\sigma}_n^\dagger \end{pmatrix}. \tag{31}$$

The above transform preserves the commutation relation of the hard-core bosons (Eq. 10), hence it is a canonical Bogoliubov transform, with details provided in the Supplemental Materials.

These $(\hat{b}_n^\dagger, \hat{b}_n)$ are the creation and annilation operators of *Bogolons*. Note that Bogolons are collective excitatons of the system, becasue (u_n, v_n) depends on Δ_n (c.f. Eq. 22), which depends on all other particles states (u_m, v_m). Under the Bogolon picture, $\hat{\mathcal{H}}$ is "diagonalize" as

$$\hat{\mathcal{H}} = \sum_n \begin{pmatrix} \hat{b}_n^\dagger & \hat{b}_n \end{pmatrix} \begin{pmatrix} E_n & 0 \\ 0 & -E_n \end{pmatrix} \begin{pmatrix} \hat{b}_n \\ \hat{b}_n^\dagger \end{pmatrix}$$

with the diagonal energy $\pm E_n$ (c.f. Eq. 23, *i.e.*, the Bogolon dispersion). The Bogoliubov canonical transform yields an equivalent result to the Schrieffer variational procedure in Eq. 20, which is a well-known result in the BCS literature.

The Gap Equation. To solve Eq. 29 and Eq. 30 analytically (with approximations), one may replace the sum by integrals: $\frac{1}{N}\sum_n f(\widetilde{\omega}_n) \to \int d\omega \mathcal{A}_\nu(\omega - \omega_0) f(\omega)$, using the normalized lineshape function (Eq. 5) as the vibrational frequency distribution function. For $g_n =$

$g_m = g_c$ special case, we have

$$\Delta(\omega) = N \int d\omega' \mathcal{A}_\nu(\omega') \left(\frac{1}{\omega - \omega_c} + \frac{1}{\omega' - \omega_c} \right) \times \frac{\hbar}{4} \frac{g_c^2 \cdot \Delta(\omega')}{\sqrt{(\hbar\omega' - \mu)^2 + [\Delta(\omega')]^2}}, \tag{32}$$

which is an integral equation. An interesting feature of this equation is that it contains the "*resonance*" behavior of the VSC experiments, which often observe that rate chances at $\omega_c \approx \omega_0$. Here, the energy gap equation exhibits this behavior due to the convolution between the line shape function $\mathcal{A}_\nu(\omega' - \omega_0)$ and the detuning function $1/[(\omega - \omega_c)(\omega' - \omega_c)]$. This might also explain why some VSC experiments [22, 24, 113, 114] have reproducibility challenges [113], likely due to the non-perfect matching between ω_c and ω_0 (either through the non-zero detuning due to the limitations of experimental conditions, or caused by the mirror fluctuations of the FP cavity [95]).

Similarly, Eq. 30 can also be replaced by integral form

$$\bar{n} = N \int d\omega \mathcal{A}_\nu(\omega - \omega_0) \frac{1}{2} \left[1 - \frac{\hbar\omega - \mu}{\sqrt{(\hbar\omega - \mu)^2 + \Delta(\omega)^2}} \right] \tag{33}$$

One can solve the integral in Eq. 33 and obtain $\mu = \mu(\Delta(\omega))$, then plugging into Eq. 32 solve the analytic expression of the gap. With detailed expressions of $\mathcal{A}_\nu$ (such as Eq. 7), one should be able to work it out.

For a simple special case, when there is no disorder in frequency, $\omega_n = \omega_0$, using Eq. 33 by setting $\mathcal{A}_\nu(\omega - \omega_0) \to \delta(\omega - \omega_0)$, we can solve

$$\mu = \hbar\omega_0 - \sqrt{\frac{1}{1 - \alpha^2}} \cdot \alpha |\Delta(\omega_0)|, \quad \alpha = \frac{N - 2\bar{n}}{N} \tag{34}$$

For $N \gg \bar{n}$, $\alpha \approx 1$, $1 - \alpha^2 \approx 4\bar{n}/N$, thus $\mu \approx \hbar\omega_0 \mp \sqrt{\bar{n}}|\Delta|/2\sqrt{N}$. This μ can be used as the initial guess and plugged into Eq. 32, to solve the $\Delta(\omega)$. The obtained $\Delta(\omega)$ can then be used and plugged into Eq. 33, to solve a refined expression of μ, and this procedure can be done iteratively, such that there is an analytic version of the SCF. In this work, we decided to keep it simple and stop at the no-disorder limit of μ in Eq. 34, and plug it into Eq. 32 *only once*, to obtain an approximate expression of $\Delta(\omega)$, discussed in the following section.

Using μ in Eq. 34 as an approximate expression, plugging it into Eq. 32, and assuming that the majority of the frequency-dependent contribution comes from the lineshape and detuning functions inside the integral, one has

$$\begin{aligned} \Delta(\omega) &= N\sqrt{1 - \alpha^2} \frac{\hbar}{4} g_c^2 \int d\omega' \mathcal{A}_\nu(\omega') \left(\frac{1}{\omega - \omega_c} + \frac{1}{\omega' - \omega_c} \right) \\ &\approx N\sqrt{e^{-\beta\hbar\omega_0}} \frac{\hbar}{2} g_c^2 \int d\omega' \mathcal{A}_\nu(\omega') \left(\frac{1}{\omega - \omega_c} + \frac{1}{\omega' - \omega_c} \right) \end{aligned} \tag{35}$$

where we have used the fact that $N\sqrt{1 - \alpha^2} \approx N\sqrt{4\bar{n}/N} \approx 2N\sqrt{e^{-\beta\hbar\omega_0}}$. Assuming $\mathcal{A}_\nu$ has a Gaussian Lineshape (Eq. 7), one can get analytic and approximate expressions for the gap (through the Dawson function type integral), resulting in the following expression with error function

$$\Delta(\omega) \approx \frac{1}{2} \hbar N g_c^2 \sqrt{e^{-\beta\hbar\omega_0}} \left[\frac{1}{\delta_\omega} + \frac{\sqrt{\pi}}{\sqrt{2}\sigma} e^{\delta_0^2/2\sigma^2} \operatorname{erfi}\left(\frac{\delta_0}{\sqrt{2}\sigma} \right) \right], \tag{36}$$

where $\operatorname{erfi}(x) = -i \operatorname{erf}(ix)$ is the imaginary error function, and we have defined $\delta_\omega = \omega - \omega_c$ and $\delta_0 = \omega_0 - \omega_c$, In the limit of small frequency disorders, *i.e.*, $|\omega_0 - \omega_c| \gg \sqrt{2}\sigma$, the above integral in Eq. 35 yields

$$\Delta(\omega) \approx N\sqrt{e^{-\beta\hbar\omega_0}} \frac{\hbar}{2} g_c^2 \left(\frac{1}{\delta_\omega} + \frac{1}{\delta_0} + \frac{\sigma^2}{\sqrt{2}\delta_0^3} \right) + \mathcal{O}\left(\frac{3\sigma^4}{\delta_0^5} \right). \tag{37}$$

In the regime $\omega_0 - \omega_c \ll \sqrt{2}\sigma$, the gap function becomes

$$\Delta(\omega) \approx \hbar N g_c^2 \sqrt{e^{-\beta\hbar\omega_0}} \left(\frac{1}{\omega - \omega_c} + \frac{\omega_0 - \omega_c}{\sigma^2} \right) + \mathcal{O}\left(\frac{\delta_0^3}{3\sigma^4} \right). \tag{38}$$

The above expression will be useful when ω is very close to ω_c, which we believe will be a macroscopic condensation and VSC effect. Detailed derivations of Eq. 36-Eq. 38 are provided in the Supplemental Materials.

For the pure-homogeneous case, one can drastically simplify the analysis, with $\omega_n = \omega_0$ for all $n \in [1, N]$. In this case, all v_n^2 are identical due to symmetry, and from Eq. 16, $v_n^2 = e^{-\beta\hbar\omega_0}$, and $u_n^2 = 1 - e^{-\beta\hbar\omega_0}$. The gap Δ_n in Eq. 22 (for all $n \in [1, N]$) becomes

$$\begin{aligned} |\Delta_n| &= \left| G \sum_{m \neq n} u_m^* v_m \right| = (N - 1)|G| \sqrt{e^{-\beta\hbar\omega_0}(1 - e^{-\beta\hbar\omega_0})} \\ &\approx N|G|\sqrt{e^{-\beta\hbar\omega_0}} \approx \frac{N\hbar g_c^2}{|\omega_0 - \omega_c|} \sqrt{e^{-\beta\hbar\omega_0}}, \end{aligned} \tag{39}$$

where we have used $N - 1 \approx N$. Indeed, when considering $\omega = \omega_0$ case of Eq. 37, $\Delta(\omega_0)$ is expressed as

$$|\Delta(\omega_0)| \approx \hbar N g_c^2 \sqrt{e^{-\beta\hbar\omega_0}} \left(\frac{1}{|\omega_0 - \omega_c|} + \frac{1}{\sqrt{2}} \frac{\sigma^2}{|\omega_0 - \omega_c|^3} \right), \tag{40}$$

and the no frequency disorder case ($\omega_n = \omega_0$) result in Eq. 39 is a special limit of Eq. 40 with $\sigma \to 0$.

Furhter, using μ expressed in Eq. 34, and the $\Delta(\omega)$ expression in Eq. 36 (or Eq. 38 for the small detuning case), we have analytic expressions for the expansion coefficients

$$u^2(\omega) = \frac{1}{2} \left[1 + \frac{\hbar\omega - \mu}{\sqrt{(\hbar\omega - \mu)^2 + \Delta(\omega)^2}} \right] \tag{41a}$$

$$v^2(\omega) = \frac{1}{2} \left[1 - \frac{\hbar\omega - \mu}{\sqrt{(\hbar\omega - \mu)^2 + \Delta(\omega)^2}} \right] \tag{41b}$$

For the VSC system that exhibits angular disorders, one needs to solve Eq. 29 and Eq. 30 numerically. Nevertheless, Eq. 29 can be formally expressed as

$$\Delta(\omega,\phi) = \frac{g_c^2}{\pi}\int_0^\pi \sin\phi'\cdot d\phi'(\cos\phi\cdot\cos\phi') \times \int d\omega' \frac{\Delta(\omega',\phi')}{\sqrt{(\hbar\omega'-\mu)^2+\Delta(\omega',\phi')^2}}, \quad (42)$$

which again, is an integral equation that requires Eq. 30 to be solved together. Note that $\int_0^\pi \sin\phi'\cdot d\phi'\cdot\cos\phi' = 0$, so one *should not* make any approximation in the integral to remove the ϕ-dependence of Δ (for example, $\Delta(\omega',\phi') \to \Delta(\omega')$ then integrate out the angle part). It is often challenging for existing theory [59, 60, 64] to explain why VSC can cause any changes in the rate constant when considering the dipole orientational disorders. More specifically, the light-matter coupling strength is $g_n = g_c\cos\phi_n$ (c.f. Eq. 9), where the angle should have an isotropic distribution, such that $\langle\cos\phi_n\cdot\cos\phi_m\rangle = \frac{1}{3}\delta_{nm}$. This leads to $\sum_{m\neq n} G_{nm} \propto \sum_{m\neq n}\cos\phi_n\cos\phi_m \to 0$. In our own opinion, this is perhaps the most difficult part to explain the VSC effects, and TST [64], classical rate theory [59], and FGR level of theory [60] all predict that there is no rate constant modification as long as one has these dipole orientational disorders. However, it is not necessarily the case for the current theory. As long as the $u_m^* v_m$ are non-uniform (having different values for different m, the gap is non-zero $\Delta_n \equiv \sum_{m\neq n} G_{nm}u_m^* v_m \neq 0$ (Eq. 22), even though $\langle\cos\phi_n\cdot\cos\phi_m\rangle = 0$ for $n \neq m$. Our initial numerical investigatons indeed show a non-zero gap when we fully consider the isotropic disorders. However, due to the random sign of these G_{nm} coupling elements, the convergence is very difficult, and future efforts are required. Altneratively, the above integral in Eq. 42 could be solved by performing an analytic type of SCF, by using the trapezoidal rule to discretize the integral in Eq. 42, togehter with Eq. 33, and then iteratively solve $\Delta(\omega_n,\phi_m)$ on a given 2D grid (ω_n,ϕ_m), iteratively, until the numerics reach self-consistency. The initial guess needs to have a non-uniform distribution in ϕ' (broken symmetry solution) in order to get the non-zero integral.

We are confident that there must be better versions of the gap equation for Eq. 32 with an analytic form (or for other lineshapes, such as for Lorentzian lineshapes), just like many different available gap equations for the BCS theory. Nevertheless, it is good to pause here and return to some simple physical pictures before continuing to search for those expressions. The typical values for the VSC experiments to achieve effects are $\Omega_R^{exp} \approx 100$ cm^{-1} when the sample has isotropic orientational disorders, and thus $\sqrt{N}g_c \approx \sqrt{3}\Omega_R^{exp}/2$, $\omega_0 \approx 1000$ cm^{-1}, $e^{-\beta\hbar\omega_0} \approx 8.2\times10^{-3}$. As such, for a detuning with $|\omega_0-\omega_c| \approx 1$ cm^{-1}, the estimated gap per quasi-particle (bogolons) using Eq. 39 is $|\Delta_n| \approx 677.8$ cm^{-1}, already surpassing room temperature thermal fluctuations $k_BT \approx 200$ cm^{-1}. The many-body picture seems to resolve the conceptual challenge faced in the single-excitation picture in VSC. In a single excitation picture, the energy gap between $|\pm\rangle$ and $\{|\mathcal{D}_j\rangle\}$ is $\Omega_R/2 = \sqrt{N}g_c \approx \sqrt{3}\Omega_R^{exp}/2 \approx 86.6$ cm^{-1} (for zero detuning $\omega_c-\omega_0 = 0$ and for $\Omega_R^{exp} \approx 100$ cm^{-1}), and typically, $\sqrt{N}g_c < k_BT$, and the dark states also have a large effective entropic contribution to the free enrgy $-k_B\ln(N-1)$, making it difficult to understand why polariton states are playing a special role in terms of VSC. In the many-body picture, the Bogolons condensed into one macroscopic state $|\widetilde{0}\rangle$, opening up an energy gap per bogolon with $\Delta_n \approx \frac{1}{4}\hbar\Omega_R^2\sqrt{e^{-\beta\hbar\omega_0}}/|\omega_0-\omega_c| \gg k_BT$, making the $|\widetilde{0}\rangle$ the special domnating state in VSC.

Condition to achieve macroscopic condensation. Due to the more stable new ground state $|\widetilde{0}\rangle$, the system condenses to this one macroscopic state. This opens up a gap between $|\widetilde{0}\rangle$ and the normal thermodynamic states of N vibrations under temperature T. For the normal thermodynamic states, its energy is

$$E_0 = N\cdot\frac{e^{-\beta\hbar\omega_0}}{1+e^{-\beta\hbar\omega_0}}\cdot\hbar\omega_0 \approx Ne^{-\beta\hbar\omega_0}\cdot\hbar\omega_0.$$

There is a dense manifold of microscopic states with entropy of $S = \ln[N!/(\bar{n}!\cdot(N-\bar{n})!)]$. The entropy for the normal state can also be evaluated using the Gibbs formula (equivalently through Stirling approximation of the Boltzmann entropy) as $\mathcal{S} = Nk_B(p_g\ln p_g + p_e\ln p_e)$ (where $p_e = e^{-\beta\hbar\omega_0}/(1+e^{-\beta\hbar\omega_0})$ and $p_g = 1/(1+e^{-\beta\hbar\omega_0})$. As such, the dense manifold of the normal excited states has a free energy that is lowered, due to the entropic contribution

$$\begin{aligned}\mathcal{F}_0 &= E_0 - T\mathcal{S} = E_0 - \left[E_0 + Nk_BT\ln\left(1+e^{-\beta\hbar\omega_0}\right)\right] \\ &= -Nk_BT\ln\left(1+e^{-\beta\hbar\omega_0}\right) \approx -Nk_BTe^{-\beta\hbar\omega_0}. \quad (43)\end{aligned}$$

Further, the vacuum state $|0\rangle$ (outside the cavity) has a free energy of $\mathcal{F}_g = 0\cdot N - T\ln 1 = 0$, and the normal manifold of states (thermaldynamics state) has a lower free energy than $|0\rangle$, thus more probable to be seen at T.

For the macroscopic state $|\widetilde{0}\rangle$, the free energy associated with this one macroscopic state is $\widetilde{\mathcal{F}}_0 = \widetilde{\mathcal{H}} - k_BT\ln 1 = \widetilde{\mathcal{H}}$, which is same as the new ground state's energy, where Δ_n is the gap for each of the phonon DOF (c.f. Eq. 21). Thus, as long as the gap surpasses the Entropic contribution of the normal states, the macroscopic BCS-type $|\widetilde{0}\rangle$ is a more favorable state for the system.

The gap for the entire N particle system is

$$\sum_{n=1}^N \Delta_n u_n v_n \approx N\Delta_n\sqrt{e^{-\beta\hbar\omega_0}} \approx \frac{N(N-1)\hbar g_c^2}{|\omega_0-\omega_c|}e^{-\beta\hbar\omega_0},$$

which scales as $\propto N^2 g_c^2$.

As such, the estimated energy for $|\widetilde{0}\rangle$ is (c.f. Eq. 15) is

$$\begin{aligned}\widetilde{\mathcal{F}}_0 = \overline{\mathcal{H}} &= \sum_n \hbar\widetilde{\omega}_n |v_n|^2 - \sum_n \Delta_n u_n v_n \\ &\approx N e^{-\beta\hbar\omega_0}\left(\hbar\omega_0 + \frac{g_c^2}{|\omega_0-\omega_c|}\right) - \frac{N(N-1)\hbar g_c^2}{|\omega_0-\omega_c|}e^{-\beta\hbar\omega_0} \\ &\approx E_0 - \frac{N(N-2)\hbar g_c^2}{|\omega_0-\omega_c|}e^{-\beta\hbar\omega_0} \approx E_0 - \frac{1}{4}\frac{N\hbar\Omega_R^2}{|\omega_0-\omega_c|}e^{-\beta\hbar\omega_0}, \\ &\approx N\hbar\omega_0 e^{-\beta\hbar\omega_0} - N^2\frac{\hbar g_c^2}{|\omega_0-\omega_c|}e^{-\beta\hbar\omega_0}\end{aligned} \tag{44}$$

where we have used $N-2\approx N$ (with the very large N considered in VSC) and $\Omega_R = 2\sqrt{N}g_c$. As one can see, the re-normalization of the frequency $\widetilde{\omega}_n$ does not impact the gap for the entire system (in terms of the orders of N).

To discover the conditions under which the new ground state $|\widetilde{0}\rangle$ has even a lower free energy than the normal state (and thus, lower than the vacuum state $|0\rangle$), $\widetilde{\mathcal{F}}_0 = \widetilde{\mathcal{H}} < \mathcal{F}_0$, one has the condition $\widetilde{\mathcal{F}}_0 = \widetilde{\mathcal{H}} < \mathcal{F}_0$ becomes

$$N\hbar\omega_0 e^{-\beta\hbar\omega_0} - \sum_n \Delta_n u_n v_n < -Nk_B T e^{-\beta\hbar\omega_0}. \tag{45}$$

Assuming that $u_n v_n \approx \sqrt{e^{-\beta\hbar\omega_0}}$, or equivalently, using μ in Eq. 34, one has

$$|\Delta_n| > \sqrt{e^{-\beta\hbar\omega_0}}\cdot(\hbar\omega_0 + k_B T), \tag{46}$$

which is the condition that the Boglon with frequency ω_n and a gap $|\Delta_n|$ shall be more stable that the normal thermodynamics phase. For the no-disordered case, using $|\Delta_n|$ expression in Eq. 39, we have

$$\hbar\Omega_R^2 > 4|\omega_0-\omega_c|\cdot(\hbar\omega_0 + k_B T). \tag{47}$$

With the frequency disorders, the above picture shows that all N molecules participate in the macroscopic state changes. This is because for a range of ω_n, the gap $\Delta(\omega_n)$ will be very different, having a very large value for $\omega_n \approx \omega_c$, and small when the detuning is large. For a system with frequency disorders, one should expect that only for those Bogolons with frequency close to ω_c would open up a large enough gap. As such, only a fraction of molecules out of N participate in the condensate state $|\widetilde{0}\rangle$. This requires that for a given frequency,

$$|\Delta(\omega)| > \sqrt{e^{-\beta\hbar\omega_0}}(\hbar\omega_0 + k_B T). \tag{48}$$

Using the approximate expression of $\Delta(\omega)$ in Eq. 38, we have the range of the frequency within which the Bogolon has a large enough gap to make it more stable than the normal thermodynamics phase. This leads to the "critical frequency" expressed as follows

$$\omega_c^{\pm} = \omega_c \pm \frac{\hbar N g_c^2}{2(\hbar\omega_0 + k_B T) - \hbar N g_c^2\cdot\Xi(\delta_0,\sigma)}, \tag{49}$$

where $\Xi(\delta_0,\sigma)$ is expressed as

$$\Xi(\delta_0,\sigma) \equiv \left|\frac{\sqrt{\pi}}{\sqrt{2}\sigma}e^{-\delta_0^2/2\sigma^2}\,\mathrm{erfi}\left(\frac{\delta_0}{\sqrt{2}\sigma}\right)\right|. \tag{50}$$

Eq. 49 means that for $\omega_n \in [\omega_c^-, \omega_c^+]$, these Bogolons are stabler than the normal thermodyanmics phase, whereas for $\omega_n < \omega_c^-$ and $\omega_n > \omega_c^+$, the Bogolons can be excited to normal phase due to their small energy gap. The numerical test of the critical frequency is provided in Fig. 1c. Note that Eq. 49 has a further approximation when we derived it, so it slightly deviates from the true intercepts between the red curve of $|\Delta(\omega)|$ and the black line $\sqrt{e^{-\beta\hbar\omega_0}}(\hbar\omega_0 + k_B T)$.

The fraction of the participating vibrations in this condensate phase (out of a total N) is thus

$$\rho = \int_{\omega_c^-}^{\omega_c^+} d\omega \mathcal{A}_\nu(\omega-\omega_0) = \int_{\omega_c^-}^{\omega_c^+} \frac{d\omega}{\sqrt{2\pi\sigma^2}}\exp\left[-\frac{(\omega-\omega_0)^2}{2\sigma^2}\right]. \tag{51}$$

Note that in either case, $|\widetilde{0}\rangle$ has a lower free energy than the normal state, as well as the vacuum state $|0\rangle$. Eq. 47 and Eq. 49-Eq. 51 are the key results of this work, which predicts the critical condition that the Bogolon Condensation in VSC cavity QED will occur with a reasonably large Ω_R, a reasonably small light-matter detuning $|\omega_0-\omega_c|$, and a reasonably low vibraitonal frequency ω_0, and could even occur at *room temperature* as most of the VSC experiments were operating [17, 21, 32, 33, 36].

Estimation Based on the Experiments. As shown in the previous work, one needs to be careful with the experimentally measured Rabi splitting, because frequency disorder also contributes to it [93, 94]. Following Ref. [93], and considering the angular disorder which reduces the effective Rabi splitting by [59, 81, 94] $1/\sqrt{(\sum_n \cos_n^2\theta)/N} = 1/\sqrt{3}$ times. The dipole angular control has been experimentally accomplished for VSC and verified [115, 116] using voltage-controlled switching [115] or temperature-controlled switching [116] of liquid crystals molecules in different alignments (*e.g.*, Fig. 3a in Ref. [116]). Combining this angular disorder together with the broadening of cavity linewidth and molecular linewidth, we have

$$\Omega_R^{\mathrm{exp}} = \frac{2}{\sqrt{3}}\,\mathrm{Im}\left[\sqrt{\frac{\gamma^2}{4} - Ng_c^2\sqrt{1+\frac{\gamma(\kappa+\gamma)}{2Ng_c^2}}}\right], \tag{52}$$

where with γ as the matter linewidth ($\gamma = 2\sigma$) and κ as the cavity linewidth, if both lineshapes are Lorentzian [93]. Using the above, the "actual" Rabi-Splitting (that report the actual light-matter coupling strength) $\Omega_R \equiv 2\sqrt{N}g_c$ is expressed

$$\Omega_R = \left[\frac{\left[\gamma^2(\kappa+\gamma)^2 + 4(3(\Omega_R^{\mathrm{exp}})^2 + \gamma^2)\right]^{1/2} - \gamma(\kappa+\gamma)}{2}\right]^{1/2}. \tag{53}$$

Numerically, we found that the detailed value of γ and κ in most of the experiments has a limited impact on $\Omega_{\rm R}$, whereas the majority impact from the $1/\sqrt{3}$ facor due to the angular disorder, such that $\Omega_{\rm R} \approx \sqrt{3}\Omega_{\rm R}^{\rm exp}$. It is thus important to emphasize that the experimentally reported Rabi splitting from linear spectra $\Omega_{\rm R}^{\rm exp}$ would be only $1/\sqrt{3}$ of the $2\sqrt{N}g_{\rm c}$, when one needs to quantitatively compare theory and experiments.

In Ref. [33] for the VSC-NMR experiment, under the concentration of 1M for the molecule, the experimentally observed Rabi splitting is $\Omega_{\rm R}^{\rm exp} \approx 83$ cm^{-1}, with cavity linewidth $\kappa = 70$ cm^{-1} and vibrational linewidth $\gamma = 2\sigma = 18$ cm^{-1}, leading to $\Omega_{\rm R} = 2\sqrt{N}g_{\rm c} \approx 142.2$ cm^{-1}. For the critical concentration at 0.5M, $\Omega_{\rm R}$ should be reduced by $\sqrt{2}$ becasue N is effectively reduced by 2 (c.f. Eq. 3), leading to the experimentally observed critical $\Omega_{\rm R} \approx 142.2/\sqrt{2} \approx 100.5$ cm^{-1}, or equivalently, $\Omega_{\rm R}^{\rm exp} \approx 58.6$ cm^{-1} at the critical concentration of 0.5M. For the no-disordered limit, the critical condition requires the detuning at an order of $|\omega_0 - \omega_{\rm c}| \approx 0.79$ cm^{-1}, and Eq. 47 predicts the same cirtical Rabi splitting to see VSC modificsation is $\Omega_{\rm R}^{\rm exp} \approx 58.6$ cm^{-1}. For the reaction reported in Ref. [17] and Ref. [18], where the rate constant suppression by up to 4.5 times is achieved when coupling cavity to Si-C vibrations. From Fig. 3D in Ref. [18], it seems that this modification only start to occur when $\Omega_{\rm R}^{\rm exp} > 55$ cm^{-1}, with no data point reported for a smaller $\Omega_{\rm R}^{\rm exp}$. In this setup, $\hbar\omega_0 = 860$ cm^{-1}, $\Omega_{\rm R}^{\rm exp} \approx 55$ cm^{-1}, $\kappa = 24.1$ cm^{-1}, $\gamma = 40$ cm^{-1}. As such, $\Omega_{\rm R} \approx 98.3$ cm^{-1}, that means $\delta_0 \approx 2.3$ cm^{-1} for this system when using Eq. 47 (and assming no frequency disorders). That means $\Omega_{\rm R}^{\rm exp} < 50$ cm^{-1} there will be no condensate.

Of course, the above estimation should be viewed, to the best, as an averaged, simplified estimation, because the expression itself does not consider any frequency and angular disorders. The real experimental systems do have frequency disorders, as well as dipole angular disorders. Instead, the real system in Ref. 33 has frequency disorder, and an estimated detuning [33] of $|\delta_0| = |\omega_{\rm c} - \omega_0| \approx 1$ cm^{-1}. Together with $\omega_0 = 2970$ cm^{-1}, $k_{\rm B}T = 200$ cm^{-1}, and the experimental critical $\Omega_{\rm R}^{\rm exp} \approx 54.8$ cm^{-1}, Eq. 49 gives that $|\omega_{\rm c}^{\pm} - \omega_{\rm c}| \approx 0.25$ cm^{-1}, meaning that only the vibrations in the frequency window of a cm^{-1} centered around $\omega_{\rm c}$ participate the condensate. Further, Eq. 51 suggests that in this window of frequency, $\rho \approx 1.1\%$, meaning 1 out of 100 of vibrations participating in the macroscopic states $|\widetilde{0}\rangle$. For $N = 10^6$ molecules, this means 10^4 of them are participating in the condensate in the Ebbesen NMR system. Interestingly, in Ref. 33, it was speculated that there would be such a phase transition. Our theory on VSC-induced Bogolon Condensation provides a concrete theoretical explanation for this phase transition behavior. For VSC rate constant measurements, there are also extensive data points provided in Ref. [21].

Eq. 47 predicts that the critical Rabi splitting to achieve the Bogolon condensation in VSC scales with $\sqrt{|\omega_0 - \omega_{\rm c}|}$, and $\sqrt{\hbar\omega_0 + k_{\rm B}T} \propto \sqrt{T}$ as well as $\sqrt{\hbar\omega_0 + k_{\rm B}T} \propto \sqrt{\hbar\omega_0} \propto \sqrt{1/M}$, where M is the effective mass for the vibrational DOF. These interesting scalings also show up in BCS-type superconductivities [86, 87], which is not surprising given that the effective Hamiltonian in Eq. 11 is mathematically isomorphic to the BCS effective Hamiltonian, and we are using the BCS-type of procedure to obtain the gap. What is interesting is that these conditions and scalings have *never* been experimentally tested in the VSC effects. So we predict that the critical $\Omega_{\rm R}$ to achieve the VSC condensation should have a $\sqrt{T}$ dependence with Temperature, as well as have a $\sqrt{1/M}$ dependence that could be checked with Isotopic/element-substitution effects.

In principle, the Moran-Ebbesen NMR experiment [33] is ideal for this test, by varying temperature and using isotopes/substitutions to change ω_0. The potential challenge to see a T-dependence of critical $\Omega_{\rm R}$ change is that it also depends on the vibrational frequency ω_0. On the other hand, it will be easier to see the isotope effect when changing C-H vibrations to C-D, which will typically reduce the frequency to $\omega_0 \approx 2100$ cm^{-1}, or even substitute the C-H vibrations to C$-^{19}$F, which has a much lower frequency of $\omega_0 \approx 1000 - 1400$ cm^{-1} and even larger vibraitonal traisition dipole. Using Eq. 47, this suggests that the C-D system ($\omega_0 \approx 2100$ cm^{-1}) will have $\Omega_{\rm R}^{\rm exp} \approx 50$ as a critical condition, and the C-F system ($\omega_0 \approx 1400$ cm^{-1}) will have $\Omega_{\rm R}^{\rm exp} \approx 41.5$ as a critical condition. For the C-F vibrations within the same Moran-Ebbesen NMR molecule, if we take $\omega_0 \approx 1400$ cm^{-1}, the current theory predicts that, if one still wants to keep $\rho = 1.1\%$, then for C-F frequency $\omega_0 \approx 1400$ cm^{-1}, and still assuming $\kappa = 70$ cm^{-1} and $\gamma = 2\sigma = 18$ cm^{-1}, the critical Rabi splitting will reduce to $\Omega_{\rm R} = 57$ cm^{-1} and $\Omega_{\rm R}^{\rm exp} = 34$ cm^{-1}. This could be tested by future experiments.

The other possible experiments are the charge-transfer complexation reaction under VSC [32], where the equilibrium constant $\mathcal{K}$ should also exhibit the same phase transition behavior if one can lower the ω_0 coupled ot the cavity. Another interesting prediction of Eq. 47 is that, for $\hbar\omega_0 \ll k_{\rm B}T$, only achieving the normal strong coupling condition (Eq. 4) will not result in condensation. There are recent experiment [117] that strongly couple the intermolecular vibrations at terahertz frequencies ($\nu = 0.5$ Thz, or $\omega_0 = 16.7$ cm^{-1}) with the cavity. The current theory (Eq. 48) predicts that unless $\Omega_{\rm R} \sim \sqrt{k_{\rm B}T} \approx 14$ cm^{-1}, there will be no VSC-induced condensation and associated effect in these Thz-VSC strong coupling systems. Similar analysis for the disordered case can be performed using Eq. 49-Eq. 51 and give valuable predictions.

How VSC impacts Chemical Kinetics? We denote k_0 as the rate constant outside the cavity, and k as the rate constant inside the cavity. Most of the experiments report k/k_0 as a function of $\omega_{\rm c} - \omega_0$, which is commonly referred to as the "action spectrum", and often found 4-5 times of rate constant reduction [17, 19, 21]

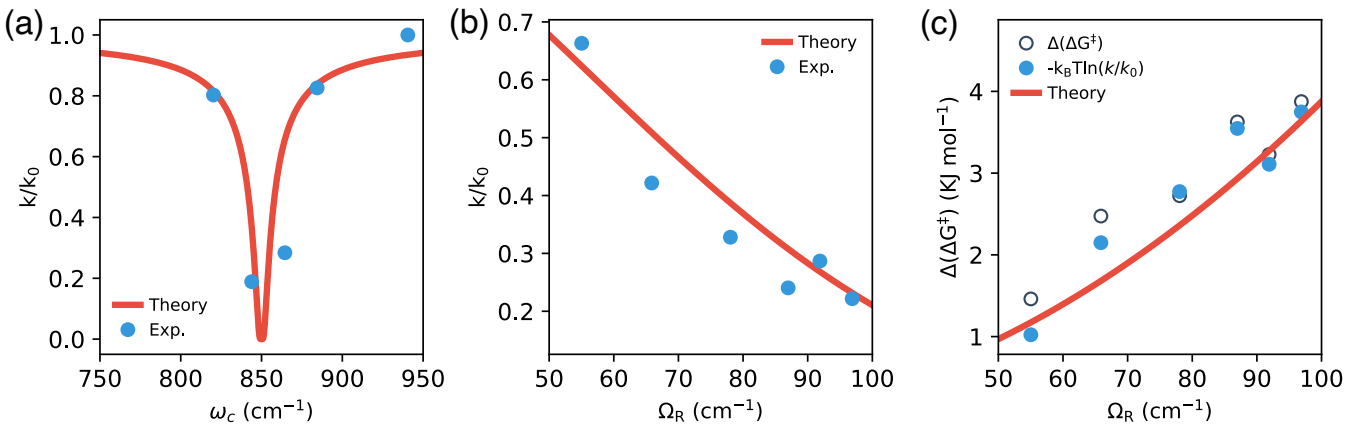

FIG. 2. **Theory and the experimental data for the rate constant modification**. A comparison of theory in Eq. 54 (red curve) with the experimentally reported data (blue dots) reproduced from Ref. [18] for the desilylation reaction of 1-phenyl2-trimethylsilylacetylene [17]. (**a**) The "action spectrum" of k/k_0 as a function of ω_c. (**b**) k/k_0 as a fucntion of Ω_R^{exp} at $|\omega_0 - \omega_c| \approx 3$ cm^{-1}. (**c**) Effective $\Delta(\Delta G^{\ddagger})$ obtained from theoy in Eq. 57, from experimetnal rate data using $-k_B T \ln(k/k_0)$ with the experimental k/k_0 (blue solid dots) as well as the $\Delta(\Delta G^{\ddagger})$ reported in Ref. [18] using a Eyring-type plot for both inside and outside cavity cases (which is a different procedure than taking $-k_B T \ln(k/k_0)$ with the experimental k/k_0).

or enhancement [22, 23, 118, 119]. Because of the macroscopic occupation of the $|\tilde{0}\rangle$ state, the system has reacted from the $|\tilde{0}\rangle$ state to the possible product states. For each Bogolon, there is an additional energy penalty Δ_n for it in order to get excited from $|\tilde{0}\rangle$, then react. As such, if we assume this is the main mechanism for the rate constant modification, we have

$$\frac{k}{k_0} = e^{-|\Delta_n|/k_B T} = \exp\left[-\frac{3\hbar \cdot \left[\Omega_R^{exp}\right]^2}{4k_B T|\omega_0 - \omega_c|} \cdot \sqrt{e^{-\beta\hbar\omega_0}}\right], \tag{54}$$

regardless of the detailed reaction mechanism outside the cavity (what is the detailed k_0 expression.

Further, Eq. 54 can be approximated through Taylor expansion

$$k/k_0 \approx 1 - \frac{3\hbar\left[\Omega_R^{exp}\right]^2}{4k_B T|\omega_0 - \omega_c|} \cdot \sqrt{e^{-\beta\hbar\omega_0}}. \tag{55}$$

We believe that this is the first time that Eq. 54 and Eq. 55 are presented in the literature. The above expression suggests that the rate constant suppression scales as $k/k_0 \propto [\Omega_R^{exp}]^2$, which was empirically observed in the Ebbesen VSC experiments (Fig. 3A in Ref. [17] or Fig. 3D in Ref. [18]). We originally thought that this quadratic scaling ought to be related to Fermi's Golden Rule [54–56, 60], which is also quadratic in coupling strength. However, those FGR faces challenges in explaining the collective effect and requires per-vibrational light-matter coupling to be as large as Ω_R^{exp}. The current theory, on the other hand, explains such quadratic scaling from a different perspective. It is because the coherent coupling among Bogolons leads to an energy gap per Bogolon, which scales as $[\Omega_R^{exp}]^2$. Further, Eq. 55 also suggests that $k/k_0 \propto |\omega_0 - \omega_c|^{-1}$, with the "width" of the peak as $3\hbar[\Omega_R^{exp}]^2\sqrt{e^{-\beta\hbar\omega_0}}/4k_B T$. This explains why the rate constant modification is sensitive to the resonance condition $\omega_c \approx \omega_0$, which is completely different than what we thought before (as photonic and vibrational energy transfer that matches lineshape relation [56]).

In experimental reports [17–19], people often assume that the rate constant still follows the Eyring-type equation, such that [18]

$$\Delta(\Delta G^{\ddagger}) \equiv \Delta G^{\ddagger} - \Delta G_0^{\ddagger} = -k_B T \ln(k/k_0). \tag{56}$$

where $\Delta G^{\ddagger}$ is the free energy barrier of the reaction inside the cavity, and $\Delta G_0^{\ddagger}$ is for outside the cavity, and please do not confuse the Δ here with our gap expressions. Note that this is not an actual change in the free-energy barrier, but rather an effective measure of the purely kinetic effect. Here, our current theory suggests that

$$\Delta(\Delta G^{\ddagger}) \approx -k_B T \ln\left(1 - \frac{3\hbar \cdot \left[\Omega_R^{exp}\right]^2}{4k_B T|\omega_0 - \omega_c|} \cdot \sqrt{e^{-\beta\hbar\omega_0}}\right). \tag{57}$$

One can see a non-linear relation of $\Delta(\Delta G^{\ddagger})$ with $\Omega_R^{(exp)}$, which has been observed experimentally [18, 20]. If one hypothesizes that an unknown mechanism forces the upper or lower vibrational polariton states to be a "gateway of VSC polaritonic chemical reactions" [62, 65], then the activation free energy change should change *linearly* [65] with Ω_R. Furthermore, in Ref. 20, it was pointed out that "a very small Rabi splitting observed in optical spectra can lead to much larger changes in activation free energy, such that $\Delta(\Delta G^{\ddagger}) > \Omega_R$, which seems to be a general trend in most VSC experiments" [17–19] and requires a theoretical explanation. Our current theory indicates that the nonlinear increase of "effective $\Delta(\Delta G^{\ddagger})$" when increasing Ω_R^{exp}, and this is due to the gap Δ_n the sys-

tem needs to overcome in order to excite the Bogolon, expressed as Eq. 57.

Fig. 2 presents a comparison of theory (Eq. 54, red curve) with the experimentally reported data (blue dots) reproduced from Ref. [18] for the desilylation reaction of 1-phenyl2-trimethylsilylacetylene [17]. Fig. 2a present the "action specturm" of k/k_0, as a function of changing ω_c. Here, we use a model parameter of $\omega_0 \approx 850$ cm^{-1}, as opposed to the original work, where there is a double peak for the vibrational transmission spectra [17, 120]. Fig. 2b presents the k/k_0 as a function of Ω_R^{exp}, using the theory in Fig. 2b and assuming a $|\omega_0 - \omega_c| \approx 3$ cm^{-1} detuning. The deviation of the experimental data from the theoretical quadratic curve is likely due to the difficulty in experimentally controlling detuning $|\omega_0 - \omega_c|$ when changing the concentration of the reactant (thus changing Ω_R^{exp}), and each experimental data point corresponds to a slightly different $|\omega_0 - \omega_c|$. Fig. 2c present the effective $\Delta(\Delta G^{\ddagger})$ obtained from theory using Eq. 56 (red curve), the experimental data converted from $-k_B T \ln(k/k_0)$ by using experimental value of k/k_0 (blue open circles), and the experimentally reported value of $\Delta(\Delta G^{\ddagger})$ by using Erying-type equation and analysis (blue dots). The theory provides a semi-quantitative agreement with the experimental data [18].

The current theory also indicates that there should also be a critical Ω_R (such as Eq. 47), upon passing it, the system starts to exhibit Bogolon condensation into $|\widetilde{0}\rangle$ and rate constant modifications. Note that the precondition to use Eq. 54 is to achieve the condensate. As such, in principle, we need to express k/k_0 in Eq. 54 as

$$\frac{k}{k_0} = \exp\left[-\frac{3\hbar\cdot\left[\Omega_R^{exp}\right]^2}{4k_B T|\omega_0-\omega_c|}\cdot\sqrt{e^{-\beta\hbar\omega_0}}\right] \cdot\Theta\left[\frac{3}{4}\hbar[\Omega_R^{exp}]^2 - |\omega_0-\omega_c|\cdot(\hbar\omega_0+k_B T)\right], \tag{58}$$

where Θ is the Heaviside step function, characterizing the condition to achieve the Bogolon condensate. This threshold, phase-transition type behavior has been observed in the charge transfer complexation reaction for equilibrium constant modification (see Eq. 60), which could also be interpreted by modifying the forward rate constant, but it has not been explicitly mentioned in the published work of VSC rate constant modifications [17, 18, 21]. Nonetheless, the reported rate constant modification always starts from a certain value of $\Omega_R^{exp} > 55$ cm^{-1}, *e.g.* in Ref. [18].

Note that Eq. 54 always leads to the rate constant *suppression*. Rate constant enhancement [22, 23, 119] would likely depend on the details of the reaction mechanism, such that the modification of $\{|u_n^2|, |v_n^2|\}$ in the frequency window $\omega \in [\omega_c^-, \omega_c^+]$ (see Fig. 1b) dictates the overall apparent rate constant. We provide a qualitative model in the Supplementary Information, but quantitative analysis is beyond the scope of the current work and will be our focus in the near future.

Why Cooperative VSC even works?. We should note that our above discussions on rate constant modifications are formulated in the context of a cavity directly coupled to vibrations of the reactant [17, 19, 21], either the reaction coordinate-related normal modes [17] or the non-reactive normal modes (spectator modes) [43, 53]. There are other types of the "cooperative vibrational strong coupling" experiments [22, 23, 118, 119] that couple the cavity mode to the solvent vibrations (with frequency ω_0), and the solvent frequency closely matches a reactive vibrational frequency ω_R in reactant molecules. Due to the low concentrations of the reactant, the strong coupling and Rabi splitting are mainly caused by cavity coupling to solvent vibrations [22].

In those cooperative coupling VSC experiments[22, 23, 118, 119], it was found that the cooperative resonant condition $\omega_c \approx \omega_0 \approx \omega_R$ is required to achieve rate constant modifications. The isotope control experiments [22, 23] could set $\omega_c \approx \omega_0 \neq \omega_R$, and there will be no obvious VSC rate constant modifications, even though a strong coupling condition between cavity and solvent is still satisfied [22, 23]. These cooperative couplings through solvent DOF have shown either rate constant suppression [118] or enhancement [22, 23, 119]. In the past, we have developed an interesting theoretical model [59] and rate constant theory [60] based on FGR to explain this phenomenon (through a mechanism of cavity-solvent strong coupling that removes the thermal vibrational excitations away from the reactant), but that theory [60] is still in the effective single excitation subspace mechanistic picture (Eq. 2). We should also note that the reaction reported in Ref. [22] was under debate, as Ref. [113] claims that there is no obvious VSC effect when trying to reproduce it, but later experimental works [24, 121] suggest that there are cooperative VSC modifications of the rate constant in different type of cavities.

With the current theory, we hypothesize that the new macroscopic state $|\widetilde{0}\rangle$ now contains both solvent vibrations and the reactant vibrations. For example, we consider a total of N solvent DOF, and a total of $\mathcal{M}$ reactant molecules (and $\mathcal{M} \ll N$ for these cooperative coupling experiments [22–24, 114, 118, 119, 121]). Through the same procedure,

$$|\widetilde{0}\rangle = \prod_{m=1}^{N+\mathcal{M}} (u_m + v_m \hat{\sigma}_m^{\dagger})|0\rangle, \tag{59}$$

the macroscopic quantum state now is a many-body states that involves both solvent and reactant molecules, a *co-condensate* of both solvent and reactant vibrational DOFs. The rate constant modification requires that the detuning is small, and thus the resonance condition $\omega_c \approx \omega_0 \approx \omega_R$. The current theory provides a possible explanation to this cooperative coupling effect as the co-condensation among the solvent and solute vibrational DOFs. Upon isotope substitution in the solvent, which makes $\omega_0 \neq \omega_R$, even though the strong coupling condition is still achieved between cavity and solvent [22, 23]

at $\omega_c \approx \omega_0$, the vibrations in the reactant molecules no longer participate in forming the macroscopic state $|\widetilde{0}\rangle$ (described by Eq. 14, as opposed to Eq. 59), and thus there is no VSC-induced rate constant modificatons. The current theory explains why the cooperative strong coupling is very sensitive to the frequency matching for the cavity, solvent, and reactant. Further numerical studies and detailed model investigations are still required in the future.

How VSC impacts Equilibrium Constant? In the VSC NMR experiment [33], Moran and Ebbesen discovered that VSC can modify the equilibrium constant $\mathcal{K}$ of the conformation change of a molecule between the unfolded configuration and a folded configuration (see Fig. 4d in Ref. [33]). Further, the equilibrium constant modification has also been shown in a charge transfer complexation reaction [32], which also exhibits a phase transition type of behavior (see Fig. 2a in Ref. [32]). These modifications on the equilibrium constant $\mathcal{K}$ were previously thought to be theoretically impossible when considering classical statistical mechanics [42, 65, 76, 122]. Explaining the VSC-induced large change of $\mathcal{K}$, which exhibits a phase transition type of behavior [32, 33] upon a critical value of Ω_R, is another challenging task in theoretical chemistry [65, 76, 122].

Our current theory provides a possible explanation for the change of $\mathcal{K}$. Let us consider a simple model for two species (diabatic electronic states) $|\mathcal{R}_n\rangle$, which couples to the vibrational DOF $(\sigma_n^\dagger, \sigma_n^\dagger)$ for the reactant, and $|\mathcal{P}_n\rangle$ for the product, and $|\mathcal{R}_n\rangle$ and $|\mathcal{P}_n\rangle$ can couple to each other through electronic coupling $\langle \mathcal{R}_n|\hat{V}|\mathcal{P}_n\rangle = \mathcal{V}$, giving two adiabatic states, with the lower energy one as the ground state that exhibit two minimum. The equilibrium constant (assuming detailed balance) can be written as

$$\mathcal{K} = \frac{[\mathcal{P}]}{[\mathcal{R}]} = \frac{k_1}{k_2}, \tag{60}$$

with k_1 describes the rate constant for the forward process and k_2 for the backward process. If the cavity only has VSC coupling to the vibrational DOFs in $|\mathcal{R}_n\rangle$, then due to the macroscopic occupation in $|\widetilde{0}\rangle$ for the vibrations on the reactant side, k_1 could be modified. If the cavity couples to both vibrational modes associated with the $|\mathcal{R}_n\rangle$ and $|\mathcal{P}_n\rangle$ states, it is also possible that k_1 and k_2 get modified in different way (or in same way but in different magnitude), causing $\mathcal{K}$ changes. After all, $\mathcal{K}$ is nothing but the ratio of two rate constants, and VSC can change rate constants.

Conclusions. In this work, we used a many-body physics approach, akin to the BCS theory, to analyze the many-body macroscopic ground state (Eq. 26) in VSC Cavity QED. We derived the Gap equation (Eq. 29, Eq. 32, and Eq. 36) that characterizes energy stabilization of the condensate state compared to the normal thermodynamic state (Eq. 47). We found that upon collective light-matter coupling, Bogolon could condense into one macroscopic state $|\widetilde{0}\rangle$ (see Eq. 26), as long as one can achieve a critical value of Ω_R (see Eq. 47). Our theory provides potential explanations for many recently observed VSC mysteries. The Moran-Ebbesen NMR experiment [33] and charge-transfer complex experiment [32] could provide direct evidence to see such a normal phase to Bogolon condensation phase, and our current theory provides a good agreement on the critical value of Ω_R to achieve the observed new phase, which agrees with the experiment [33].

The current theory has several predictions that could be experimentally verified. One of the most important predictions is the condition to achieve the Bogolon condensation phase, which requires a critical Ω_R (Eq. 47). This phase transition type of behavior has already been observed in the NMR experiment [33], the charge-transfer complexation reaction experiments [32], and should also be observed in the VSC-modification of rate constants [18, 21]. One possibility is to use the recently reported reactions in Ref. [21], and gradually reduce the Ω_R, one should observe a null kinetic effect of VSC. Our theory gives quantitative predictions for the critical Ω_R needed to achieve the Bogolon condensate, and thus VSC-induced modifications. More generally, the critical condition is $\Omega_R \propto \sqrt{\hbar\omega_0 + k_B T}$, which could be checked by multiple known VSC experiments [17–19]. Further, the current theory (Eq. 47) also predicts that the condensation condition is very sensitive to the cavity-vibration frequency detuning $|\omega_c - \omega_0|$, which likely explains why some VSC experiments [22, 24, 113, 114, 121] have issues on the reproducibility [113] due to the non-perfect matching between ω_c and ω_0 (either through the non-zero detuning, or caused by the mirror fluctuations of the FP cavity [95]).

Our theory also obtain possible explanations for the VSC rate constant modifications due to the fact that the system needs extra thermal energy to excite Bogolon. This leads to our rate constant theory in Eq. 54 or Eq. 55, which predicts the quadraic dependence $k/k_0 \propto [\Omega_R^{\rm exp}]^2$. As a corollary, the effective $\Delta(\Delta G^\ddagger) = -k_B T \ln(k/k_0)$ scales non-linearly with $\Omega_R^{\rm exp}$. The rate constant modification also scales as Eq. 55 also suggests that $k/k_0 \propto |\omega_0 - \omega_c|^{-1}$, with the "width" of the peak as $3\hbar[\Omega_R^{\rm exp}]^2\sqrt{e^{-\beta\hbar\omega_0}}/4k_B T$. Comparing with the experimental data reported in Ref. [18], our theory seems to provide a reasonable semi-quantitative agreement with all trends, with nearly no free parameter ($|\omega_0 - \omega_c|$ is viewed as a free parameter, which is difficult to read out and control from the experiments). This also means the future experimental platform could focus on cavity structures that provide stable light-matter detuning $|\omega_0 - \omega_c|$, which is the key for k/k_0 reproducibility and data consistency, as suggested by the current theory (Eq. 55). The recent experimental work [24] on using the non-local metasurfaces cavity could be a good starting point.

Similarly, one can qualitatively understand the cooperative VSC rate constant effects and the change of equilibrium constant from the Bogolon condensation picture, although detailed reaction models are required to

construct a quantitative argument. Assuming that the VSC-induced effects originate from one macroscopic state could also pave the way to understanding other mysterious effects. For example, why could vibrational symmetry also have a big impact on the VSC effect [38]? It could be explained because this one macroscopic state that dominates the VSC system's behavior should be sensitive to the vibrational symmetry of each single particle state, which are the building blocks of this macroscopic state. Why VSC can significantly enhance the conductivities [39] could also be potentially explained by the macroscopic occupation of the Bogolon condensation that impacts how electrons are transported through the phonon environments. The phase transition type of behavior in VSC-impacted polymerizations could also be explained by the macroscopic occupation of the $|\widetilde{0}\rangle$.

Our theoretical analysis leads to the conclusion that the mystery of VSC modifications observed in experiments could arise from a many-body quantum mechanical effect: the Bogolon condensation into one macroscopic state, or the macroscopic occupation of one state $|\widetilde{0}\rangle$. This state is non-local and macroscopic. This is why the previous theoretical effects [42, 64], including our own [54–56], can not explain the collective effect, because this macroscopic state can not be obtained perturbatively from a few-body solution [86]. A clear mechanistic understanding of VSC could elevate our knowledge of chemistry to a new era that goes beyond the traditional intuitive paradigm, which often involves *only the local barrier crossing* at the individual molecular scale. Similarly, this work brings the many-body physics picture into the cavity QED and quantum optics community, which traditionally focuses on few-body excitations (Eq. 2, due to the use of the exciton-polariton system). We hope that we have provided the first possible candidate for the *universal* theory to explain nearly all VSC Cavity QED effects and offer valuable insights. If eventually verified by experiments (*e.g.*, our theoretical predictions on critical $\Omega_{\mathrm{R}} \propto \sqrt{\omega_0}$ through isotop/substitution experiments, or the rate constant scalings with different factors), our work suggests that VSC Cavity QED is an experimental platform that actually generate yet another type of Bogolon Condensation and macroscopic quantum state, in addition to the well-known Bose–Einstein (BEC) condensates, superconductivity, and superfluidity. As opposed to the other condensates and macroscopic states, which often require very low temperatures to achieve, the VSC Bogolon condensations occur at room temperature.

ACKNOWLEDGEMENTS

This work was supported by the Air Force Office of Scientific Research (AFOSR) under Award No. FA9550-23-1-0438. M.E.M. appreciates the support from the Agnes M. and George Messersmith Fellowship by the University of Rochester. S.M.V. appreciates the support of the Elon Huntington Hooker Fellowship from the University of Rochester. Computing resources were provided by the Center for Integrated Research Computing (CIRC) at the University of Rochester. We appreciate valuable comments from Chaitanya Murthy on BSC theory and our derivations. We also appreciate valuable discussions with Maciej Piejko, Sinan Bascil, and Joseph Moran on interpreting the VSC-NMR experiments.

REFERENCES

[1] J. Hopfield, Theory of the contribution of excitons to the complex dielectric constant of crystals, Phys. Rev. **112**, 1555 (1958).

[2] M. Brune, E. Hagley, J.-M. Raimond, S. Haroche, *et al.*, Observing the progressive decoherence of the "meter" in a quantum measurement, Physical Review Letters **77**, 4887 (1996).

[3] S. M. Dutra, *Cavity Quantum Electrodynamics: The Strange Theory of Light in a Box*, Wiley Series in Lasers and Applications, Vol. 10 (Wiley, Hoboken, NJ, 2004) p. 408.

[4] S. Haroche and J.-M. Raimond, Cavity quantum electrodynamics, Scientific American **268**, 54 (1993).

[5] D. G. Lidzey, D. D. C. Bradley, M. S. Skolnick, T. Virgili, S. Walker, and D. M. Whittaker, Strong exciton–photon coupling in an organic semiconductor microcavity, Nature **395**, 53 (1998).

[6] D. G. Lidzey, D. D. C. Bradley, T. Virgili, A. Armitage, M. S. Skolnick, and S. Walker, Room temperature polariton emission from strongly coupled organic semiconductor microcavities, Physical Review Letters **82**, 3316 (1999).

[7] D. G. Lidzey, D. D. C. Bradley, A. Armitage, S. Walker, and M. S. Skolnick, Photon-mediated hybridization of frenkel excitons in organic semiconductor microcavities, Science **288**, 1620 (2000).

[8] R. J. Holmes and S. R. Forrest, Strong exciton–photon coupling and exciton hybridization in a thermally evaporated polycrystalline film of an organic small molecule, Physical Review Letters **93**, 186404 (2004).

[9] S. Kéna-Cohen, M. Davanço, and S. R. Forrest, Strong exciton-photon coupling in an organic single crystal microcavity, Physical Review Letters **101**, 116401 (2008).

[10] D. Polak, R. Jayaprakash, T. P. Lyons, L. Martínez-Martínez, A. Leventis, K. J. Fallon, H. Coulthard, D. G. Bossanyi, K. Georgiou, A. J. Petty II, J. Anthony, H. Bronstein, J. Yuen-Zhou, A. I. Tartakovskii, J. Clark, and A. J. Musser, Manipulating molecules with strong coupling: harvesting triplet excitons in organic exciton microcavities, Chemical Science **11**, 343 (2020).

[11] L. Qiu, A. Mandal, O. Morshed, M. T. Meidenbauer, W. Girten, P. Huo, A. N. Vamivakas, and T. D. Krauss, Molecular polaritons generated from strong coupling between CdSe nanoplatelets and a dielectric optical cavity, J. Phys. Chem. Lett. **12**, 5030 (2021).

[12] M. Amin, E. R. Koessler, O. Morshed, F. Awan, N. M. B. Cogan, R. Collison, T. M. Tumiel, W. Girten, C. Leiter, A. N. Vamivakas, P. Huo, and T. D. Krauss, Cavity controlled upconversion in cdse nanoplatelet polaritons, ACS Nano **18**, 21388 (2024).

[13] A. Shalabney, J. George, J. Hutchison, G. Pupillo, C. Genet, and T. W. Ebbesen, Coherent coupling of molecular resonators with a microcavity mode, Nat. Commun. **6**, 5981 (2015).

[14] J. George, A. Shalabney, J. A. Hutchison, C. Genet, and T. W. Ebbesen, Liquid-phase vibrational strong coupling, J. Phys. Chem. Lett. **6**, 10271031 (2015).

[15] J. P. Long and B. S. Simpkins, Coherent coupling between a molecular vibration and fabryperot optical cavity to give hybridized states in the strong coupling limit, ACS Photonics **2**, 130 (2015).

[16] S. Kena-Cohen and J. Yuen-Zhou, Polariton chemistry: Action in the dark, ACS Cent. Sci. **5**, 386388 (2019).

[17] A. Thomas, J. George, A. Shalabney, M. Dryzhakov, S. J. Varma, J. Moran, T. Chervy, X. Zhong, E. Devaux, C. Genet, J. A. Hutchison, and T. W. Ebbesen, Ground-state chemical reactivity under vibrational coupling to the vacuum electromagnetic field, Angew. Chem. Int. Ed. **55**, 11462 (2016).

[18] A. Thomas, A. Jayachandran, L. Lethuillier-Karl, R. M. Vergauwe, K. Nagarajan, E. Devaux, C. Genet, J. Moran, and T. W. Ebbesen, Ground state chemistry under vibrational strong coupling: dependence of thermodynamic parameters on the rabi splitting energy, Nanophotonics **9**, 249 (2020).

[19] K. Hirai, R. Takeda, J. A. Hutchison, and H. Uji-i, Modulation of prins cyclization by vibrational strong coupling, Angew. Chem. Int. Ed. **59**, 5332 (2020).

[20] K. Hirai, J. A. Hutchison, and H. Uji-i, Recent progress in vibropolaritonic chemistry, ChemPlusChem **85**, 1981 (2020).

[21] W. Ahn, J. F. Triana, F. Recabal, F. Herrera, and B. S. Simpkins, Modification of ground-state chemical reactivity via light–matter coherence in infrared cavities, Science **380**, 1165 (2023).

[22] J. Lather, P. Bhatt, A. Thomas, T. W. Ebbesen, and J. George, Cavity catalysis by cooperative vibrational strong coupling of reactant and solvent molecules, Angew. Chem. Int. Ed. **58**, 10635 (2019).

[23] J. Lather and J. George, Improving enzyme catalytic efficiency by co-operative vibrational strong coupling of water, J. Phys. Chem. Lett. **12**, 379 (2020).

[24] F. Verdelli, Y.-C. Wei, K. Joseph, M. S. Abdelkhalik, G. Masoumeh, S. H. C. Askes, A. Baldi, E. W. Meijer, and J. G. Rivas, Polaritonic Chemistry Enabled by Non-Local Metasurfaces, Angew. Chem. Int. Ed. **63**, e20240952 (2024).

[25] T.-T. Chen, M. Du, Z. Yang, J. Yuen-Zhou, and W. Xiong, Cavity-enabled enhancement of ultrafast intramolecular vibrational redistribution over pseudorotation, Science **378**, 790 (2022).

[26] G. Yin, T. Liu, L. Zhang, T. Sheng, H. Mao, and W. Xiong, Overcoming energy disorder for cavity-enabled vibrational polaritons, Science **389**, 845 (2025).

[27] T. E. Li, A. Nitzan, and J. E. Subotnik, Collective vibrational strong coupling effects on molecular vibrational relaxation and energy transfer: Numerical insights via cavity molecular dynamics simulations, Angew. Chem. Int. Ed. **60**, 15533 (2021).

[28] T. E. Li and S. Hammes-Schiffer, Qm/mm modeling of vibrational polariton induced energy transfer and chemical dynamics, Journal of the American Chemical Society **145**, 377 (2022).

[29] J. Cao, Generalized resonance energy transfer theory: Applications to vibrational energy flow in optical cavities, J. Phys. Chem. Lett. **13**, 10943 (2022).

[30] X. Li, A. Mandal, and P. Huo, Theory of mode-selective chemistry through polaritonic vibrational strong coupling, J. Phys. Chem. Lett. **12**, 6974 (2021).

[31] A. Thomas, L. Lethuillier-Karl, K. Nagarajan, R. M. A. Vergauwe, J. George, T. Chervy, A. Shalabney, E. Devaux, C. Genet, J. Moran, and T. W. Ebbesen, Tilting a ground-state reactivity landscape by vibrational strong coupling, Science **363**, 615 (2019).

[32] Y. Pang, A. Thomas, K. Nagarajan, R. M. A. Vergauwe, K. Joseph, B. Patrahau, K. Wang, C. Genet, and T. W. Ebbesen, On the role of symmetry in vibrational strong coupling: The case of charge-transfer complexation, Angew. Chem. Int. Ed. **59**, 10436 (2020).

[33] B. Patrahau, M. Piejko, R.J.Mayer, C.Antheaume, T.Sangchai, G.Ragazzon, A.Jayachandran, E.Devaux, C.Genet, J. Moran, and T. W. Ebbesen, Direct observation of polaritonic chemistry by nuclear magnetic resonance spectroscopy, Angew. Chem. Int. Ed. **63**, e202401368 (2024).

[34] K. Joseph, S. Kushida, E. Smarsly, D. Ihiawakrim, A. Thomas, G. L. Paravicini-Bagliani, K. Nagarajan, R. Vergauwe, E. Devaux, O. Ersen, U. H. F. Bunz, and T. W. Ebbesen, Supramolecular assembly of conjugated polymers under vibrational strong coupling, Angewandte Chemie International Edition **60**, 19665 (2021).

[35] K. Sandeep, K. Joseph, J. Gautier, K. Nagarajan, M. Sujith, K. G. Thomas, and T. W. Ebbesen, Manipulating the self-assembly of phenyleneethynylenes under vibrational strong coupling, The Journal of Physical Chemistry Letters **13**, 1209 (2022).

[36] K. Joseph, B. De Waal, S. A. H. Jansen, J. J. B. Van Der Tol, G. Vantomme, and E. W. Meijer, Consequences of vibrational strong coupling on supramolecular polymerization of porphyrins, Journal of the American Chemical Society **146**, 12130 (2024).

[37] S. Imai, T. Hamada, M. Nozaki, T. Fujita, M. Takahashi, Y. Fujita, K. Harano, H. Uji-i, A. Takai, and K. Hirai, Accessing a hidden pathway to supramolecular toroid through vibrational strong coupling, Journal of the American Chemical Society **147**, 23528 (2025), published online May 29, 2025.

[38] A. Jayachandran, B. Patrahau, J. G. Ricca, M. K. Mahato, Y. Pang, K. Nagarajan, A. Thomas, C. Genet, and T. W. Ebbesen, A phenomenological symmetry rule for chemical reactivity under vibrational strong coupling, Angew. Chem. Int. Ed. **64**, e202503915 (2025).

[39] S. Kumar, S. Biswas, U. Rashid, K. S. Mony, G. Chandrasekharan, F. Mattiotti, R. M. A. Vergauwe, D. Hagenmuller, V. Kaliginedi, and A. Thomas, Extraordinary electrical conductance through amorphous non-conducting polymers under vibrational strong coupling,

Journal of the American Chemical Society **146**, 18999 (2024).
[40] J. A. Campos-Gonzalez-Angulo, Y. R. Poh, M. Du, and J. Yuen-Zhou, Swinging between shine and shadow: Theoretical advances on thermally activated vibropolaritonic chemistry, J. Chem. Phys. **158**, 230901 (2023).
[41] A. Mandal, M. A. Taylor, B. M. Weight, E. R. Koessler, X. Li, and P. Huo, Theoretical advances in polariton chemistry and molecular cavity quantum electrodynamics, Chem. Rev. **123**, 9786 (2023).
[42] X. Li, A. Mandal, and P. Huo, Cavity frequency-dependent theory for vibrational polariton chemistry, Nat. Commun. **12**, 1315 (2021).
[43] C. Schäfer, J. Flick, E. Ronca, P. Narang, and A. Rubio, Shining light on the microscopic resonant mechanism responsible for cavity-mediated chemical reactivity, Nat. Commun. **13**, 7817 (2021).
[44] P.-Y. Yang and J. Cao, Quantum effects in chemical reactions under polaritonic vibrational strong coupling, J. Phys. Chem. Lett. **12**, 9531 (2021).
[45] S. Mondal, D. S. Wang, and S. Keshavamurthy, Dissociation dynamics of a diatomic molecule in an optical cavity, J. Chem. Phys. **157**, 244109 (2022).
[46] L. P. Lindoy, A. Mandal, and D. R. Reichman, Quantum dynamical effects of vibrational strong coupling in chemical reactivity, Nat. Commun. **14**, 2733 (2023).
[47] J. P. Philbin, Y. Wang, P. Narang, and W. Dou, Chemical reactions in imperfect cavities: Enhancement, suppression, and resonance, J. Phys. Chem. C **126**, 14908 (2022).
[48] D. S. Wang, T. Neuman, S. F. Yelin, and J. Flick, Cavity-modified unimolecular dissociation reactions via intramolecular vibrational energy redistribution, J. Phys. Chem. Lett. **13**, 3317 (2022).
[49] J. Sun and O. Vendrell, Suppression and enhancement of thermal chemical rates in a cavity, J. Phys. Chem. Lett. **13**, 4441 (2022).
[50] S. Mondal and S. Keshavamurthy, Phase space perspective on a model for isomerization in an optical cavity, J. Chem. Phys. **159**, 074106 (2023).
[51] S. Mondal and S. Keshavamurthy, Cavity induced modulation of intramolecular vibrational energy flow pathways, J. Chem. Phys. **161**, 194302 (2024).
[52] L. P. Lindoy, A. Mandal, and D. R. Reichman, Investigating the collective nature of cavity-modified chemical kinetics under vibrational strong coupling, Nanophotonics doi:10.1515/nanoph-2024-0026 (2024).
[53] C. Schäfer, J. Fojt, E. Lindgren, and P. Erhart, Machine Learning for Polaritonic Chemistry:Accessing Chemical Kinetics, J. Am. Chem. Soc. **146**, 5402 (2024).
[54] W. Ying and P. Huo, Resonance theory and quantum dynamics simulations of vibrational polariton chemistry, J. Chem. Phys. **159**, 084104 (2023).
[55] W. Ying, M. Taylor, and P. Huo, Resonance theory of vibrational polariton chemistry at the normal incidence, Nanophotonics **13**, 2601 (2024).
[56] W. Ying and P. Huo, Resonance theory of vibrational strong coupling enhanced polariton chemistry and the role of photonic mode lifetime, Commun. Mater. **5**, 110 (2024).
[57] J. A. Campos-Gonzalez-Angulo, R. F. Ribeiro, and J. Yuen-Zhou, Resonant catalysis of thermally activated chemical reactions with vibrational polaritons, Nat. Commun. **10**, 4685 (2019).
[58] M. Du and J. Yuen-Zhou, Catalysis by dark states in vibropolaritonic chemistry, Phys. Rev. Lett. **128**, 096001 (2022).
[59] A. Mandal, X. Li, and P. Huo, Theory of vibrational polariton chemistry in the collective coupling regime, J. Chem. Phys. **156**, 014101 (2022).
[60] S. M. Vega, W. Ying, and P. Huo, Theoretical Insights into the Resonant Suppression Effect in Vibrational Polariton Chemistry, J. Am. Chem. Soc. **147**, 19727–19737 (2025).
[61] E. Suyabatmaz, G. J. R. Aroeira, and R. F. Ribeiro, Polaritonic control of blackbody infrared radiative dissociation, The Journal of Physical Chemistry Letters **16**, 7530 (2025).
[62] H. Hiura, A. Shalabney, and J. George, A reaction kinetic model for vacuum-field catalysis based on vibrational light-matter coupling, ChemRxiv (2019).
[63] V. P. Zhdanov, Vacuum field in a cavity, light-mediated vibrational coupling, and chemical reactivity, Chem. Phys. **535**, 110767 (2020).
[64] J. A. Campos-Gonzalez-Angulo and J. Yuen-Zhou, Polaritonic normal modes in transition state theory, J. Chem. Phys. **152**, 161101 (2020).
[65] T. E. Li, A. Nitzan, and J. E. Subotnik, On the origin of ground-state vacuum-field catalysis: Equilibrium consideration, J. Chem. Phys. **152**, 234107 (2020).
[66] M. Du, Y. R. Poh, and J. Yuen-Zhou, Vibropolaritonic reaction rates in the collective strong coupling regime: Pollak–grabert–hänggi theory, J. Phys. Chem. C **127**, 5230 (2023).
[67] P. Fowler-Wright, B. W. Lovett, and J. Keeling, Efficient many-body non-markovian dynamics of organic polaritons, Physical Review Letters **129**, 173001 (2022).
[68] D. S. Wang, J. Flick, and S. F. Yelin, Chemical reactivity under collective vibrational strong coupling, J. Chem. Phys. **157**, 224304 (2022).
[69] H.-T. Chen, Z. Zhou, M. Sukharev, J. E. Subotnik, and A. Nitzan, Interplay between disorder and collective coherent response: Superradiance and spectral motional narrowing in the time domain, Phys. Rev. A. **106**, 053703 (2022).
[70] J. Sun and O. Vendrell, Modification of thermal chemical rates in a cavity via resonant effects in the collective regime, The Journal of Physical Chemistry Letters **14**, 8397 (2023), published online 2023 Sep 14.
[71] D. Sidler, M. Ruggenthaler, C. Schäfer, E. Ronca, and A. Rubio, A perspective on ab initio modeling of polaritonic chemistry: The role of non-equilibrium effects and quantum collectivity, J. Chem. Phys. **156**, 230901 (2022).
[72] D. Sidler, T. Schnappinger, A. Obzhirov, M. Ruggenthaler, M. Kowalewski, and A. Rubio, Unraveling a cavity induced molecular polarization mechanism from collective vibrational strong coupling, J. Phys. Chem. Lett. **15**, 5208 (2024).
[73] T. Schnappinger, D. Sidler, M. Ruggenthaler, A. Rubio, and M. Kowalewski, Cavity born–oppenheimer hartree–fock ansatz: Light–matter properties of strongly coupled molecular ensembles, Journal of Physical Chemistry Letters **14**, 8024 (2023), published online 2023 Aug 31.
[74] D. Sidler, M. Ruggenthaler, and A. Rubio, Collectively-modified inter-molecular electron correlations: The connection of polaritonic chemistry and spin glass physics,

arXiv arXiv:2409.08986 (2025).
[75] Y. Ke and J. O. Richardson, Insights into the mechanisms of optical cavity-modified ground-state chemical reactions, J. Chem. Phys. **160**, 224704 (2024).
[76] A. C. Hunt, Chemical reaction dynamics under vibrational strong coupling (2024).
[77] V. Rokaj, I. Tutunnikov, and H. R. Sadeghpour, Cavity-mediated collective resonant suppression of local molecular vibrations, J. Phys. Chem. Lett. **16**, 6249 (2025).
[78] B. Gu, Toward collective chemistry under strong light–matter coupling, The Journal of Physical Chemistry Letters **16**, 317 (2025).
[79] L. Borges, T. Schnappinger, and M. Kowalewski, Impact of dark polariton states on collective strong light–matter coupling in molecules, The Journal of Physical Chemistry Letters **16**, 7807 (2025).
[80] M. Tavis and F. W. Cummings, Approximate solutions for an n-molecule-radiation-field hamiltonian, Phys. Rev. **188**, 692 (1969).
[81] R. Houdré, R. P. Stanley, and M. Ilegems, Vacuum-field Rabi splitting in the presence of inhomogeneous broadening: Resolution of a homogeneous linewidth in an inhomogeneously broadened system, Phys. Rev. A **53**, 2711 (1996).
[82] J. del Pino, J. Feist, and F. J. Garcia-Vidal, Quantum theory of collective strong coupling of molecular vibrations with a microcavity mode, New J. Phys. **17**, 053040 (2015).
[83] G. D. Scholes, C. A. DelPo, and B. Kudisch, Entropy Reorders Polariton States, J. Phys. Chem. Lett. **11**, 6389 (2020).
[84] N. Bogolubov, On the theory of superfluidity, Journal of Physics **XI**, 23 (1947).
[85] L. Landau, On the theory of superfluidity, Phys. Rev. **75**, 884 (1949).
[86] J. Bardeen, L. N. Cooper, and J. R. Schrieffer, Microscopic Theory of Superconductivity, Phys. Rev. **106**, 162 (1957).
[87] J. Bardeen, L. N. Cooper, and J. R. Schrieffer, Theory of Superconductivity, Phys. Rev. **108**, 1175 (1957).
[88] J. R. Schrieffer and P. A. Wolff, Relation between the anderson and kondo hamiltonians, Physical Review **149**, 491 (1966).
[89] T. Lancaster and S. J. Blundell, *Quantum field theory for the gifted amateur* (OUP Oxford, 2014).
[90] K. S. U. Kansanen and T. T. Heikkilä, Cavity-induced bifurcation in classical rate theory, SciPost Phys. **16**, 025 (2024).
[91] S. Pannir-Sivajothi, J. A. Campos-Gonzalez-Angulo, L. A. Martínez-Martínez, S. Sinha, and J. Yuen-Zhou, Driving chemical reactions with polariton condensates, Nature Comm. **13**, 1645 (2022).
[92] K. Schwennicke, A. Koner, J. B. Perez-Sanchez, W. Xiong, N. C. Giebink, M. L. Weichman, and J. Yuen-Zhou, Unlocking delocalization: how much coupling strength is required to overcome energy disorder in molecular polaritons?, Chem. Sci. **16**, 4676 (2025).
[93] K. Schwennicke, N. C. Giebink, and J. Yuen-Zhou, enExtracting accurate light–matter couplings from disordered polaritons, Nanophotonics **13**, 2469–2478 (2024).
[94] Z. Zhou, H.-T. Chen, J. E. Subotnik, and A. Nitzan, Interplay between disorder, local relaxation, and collective behavior for an ensemble of emitters outside versus inside a cavity, Phys. Rev. A. **108**, 023708 (2023).
[95] M. A. Michon and B. S. Simpkins, Impact of cavity length non-uniformity on reaction rate extraction in strong coupling experiments, Journal of the American Chemical Society **146**, 30596 (2024), published October 28, 2024; E-pub ahead of print Nov 6, 2024.
[96] P. A. Thomas and W. L. Barnes, Strong coupling-induced frequency shifts of highly detuned photonic modes in multimode cavities, J. Chem. Phys. **160**, 204303 (2024).
[97] L. N. Cooper, Bound electron pairs in a degenerate fermi gas, Physical Review **104**, 1189 (1956).
[98] J. Bardeen and D. Pines, Electron-phonon interaction in metals, Physical Review **99**, 1140 (1955).
[99] H. Fröhlich, Interaction of electrons with lattice vibrations, Proceedings of the Royal Society of London. Series A, Mathematical and Physical Sciences **215**, 291 (1952).
[100] M. Kumar, S. Chatterjee, R. Paul, and S. Puri, Ordering kinetics in the random bond xy model, Physical Review E **96**, 042127 (2017).
[101] O. Castaños, E. López-Moreno, and J. G. Hirsch, Classical and quantum phase transitions in the lipkin–meshkov–glick model, Physical Review B **74**, 104118 (2006).
[102] D. A. Garanin, E. M. Chudnovsky, and T. Proctor, Random field xy model in three dimensions, Physical Review B **88**, 014420 (2013).
[103] A. L. Burin, Localization in a random xy model with long-range interactions, Physical Review B **92**, 104428 (2015).
[104] H. J. Lipkin, N. Meshkov, and A. J. Glick, Validity of many-body approximation methods for a solvable model (i). exact solutions and perturbation theory, Nuclear Physics **62**, 188 (1965).
[105] A. J. Glick, H. J. Lipkin, and N. Meshkov, Validity of many-body approximation methods for a solvable model (iii). diagram summations, Nuclear Physics **62**, 211 (1965).
[106] N. Debergh and F. Stancu, On the exact solutions of the lipkin–meshkov–glick model, Journal of Physics A: Mathematical and General **34**, 3265 (2001).
[107] O. Castaños, E. López-Moreno, and J. G. Hirsch, Classical and quantum phase transitions in the lipkin–meshkov–glick model, Physical Review B **74**, 104118 (2006).
[108] G. Parisi, Infinite number of order parameters for spin-glasses, Physical Review Letters **43**, 1754 (1979).
[109] G. Parisi, Spin glasses and fragile glasses: Statics, dynamics, and complexity, Proceedings of the National Academy of Sciences **103**, 7948 (2006).
[110] G. Parisi, Nobel lecture: Multiple equilibria, Reviews of Modern Physics **95**, 030501 (2023).
[111] J. M. Kosterlitz, D. J. Thouless, and R. C. Jones, Spherical model of a spin-glass, Physical Review Letters **36**, 1217 (1976).
[112] P. Pulay, Convergence acceleration of iterative sequences. the case of scf iteration, Chemical Physics Letters **73**, 393–398 (1980).
[113] G. D. Wiesehan and W. Xiong, Negligible rate enhancement from reported cooperative vibrational strong coupling catalysis, The Journal of Chemical Physics **155**, 241103 (2021).
[114] J. Singh, J. Lather, and J. George, Solvent dependence on cooperative vibrational strong coupling and cavity

catalysis, ChemPhysChem **24**, e202300016 (2023).
[115] M. Hertzog, P. Rudquist, J. A. Hutchison, J. George, T. W. Ebbesen, and K. Börjesson, Voltage-controlled switching of strong light–matter interactions using liquid crystals, Chem. Eur. J. **23**, 18166 (2017).
[116] G. Stemo, H. Yamada, H. Katsuki, and H. Yanagi, Influence of vibrational strong coupling on an ordered liquid crystal, J. Phys. Chem. B **126**, 9399 (2022).
[117] R. Damari, O. Weinberg, D. Krotkov, E. Bordo, A. Golombek, T. Schwartz, and S. Fleischer, Strong coupling of collective intermolecular vibrations in lactose to a terahertz cavity mode, Nature Communications **10**, 3248 (2019).
[118] R. M. A. Vergauwe, A. Thomas, K. Nagarajan, A. Shalabney, J. George, T. Chervy, M. Seidel, E. Devaux, V. Torbeev, and T. W. Ebbesen, Modification of enzyme activity by vibrational strong coupling of water, Angew. Chem. Int. Ed. **58**, 15324 (2019).
[119] J. Lather, A. N. K. Thabassum, J. Singh, and J. George, Cavity catalysis: modifying linear free-energy relationship under cooperative vibrational strong coupling, Chem. Sci. **13**, 195 (2022).
[120] C. Climent and J. Feist, On the s_N2 reactions modified in vibrational strong coupling experiments: reaction mechanisms and vibrational mode assignments, Physical Chemistry Chemical Physics **22**, 23545 (2020).
[121] J. Lian, Y. Song, Q. Si, X. Zhao, H. Peng, J. Hu, L. Wang, W. Zhang, and Y. Zhao, Continuous-flow fabry–pérot cavity for enhanced catalysis via cooperative vibrational strong coupling, ACS Photonics **12**, 3557 (2025).
[122] K. Sun and R. F. Ribeiro, Theoretical formulation of chemical equilibrium under vibrational strong coupling, Nature Comm **15**, 2405 (2024).